Human KDMQLGRLHMKTLLPVSK

Pan troglodytes
Identities = 18/18 (100%)

Query 1 KDMQLGRLHMKTLLPVSK 18
KDMQLGRLHMKTLLPVSK
Sbjct 751 KDMQLGRLHMKTLLPVSK 768

Macaca mulatta
Identities = 17/18 (94%)

Query 1 KDMQLGRLHMKTLLPVSK 18
KD+QLGRLHMKTLLPVSK
Sbjct 745 KDLQLGRLHMKTLLPVSK 762

Bos taurus
Identities = 14/18 (77%)

Query 1 KDMQLGRLHMKTLLPVSK 18
K+MQLGRLH+K+LLPV+K
Sbjct 745 KNMQLGRLHIKSLLPVTK 762

Sus scrofa
Identities = 12/16 (75%)

Query 1 KDMQLGRLHMKTLLPV 16
K++QLGRLH+KTLL V
Sbjct 745 KNIQLGRLHIKTLLAV 760

Mus musculus
Identities = 12/15 (80%)

Query 4 QLGRLHMKTLLPVSK 18
QLGR+H+KTLLPV K
Sbjct 666 QLGRIHIKTLLPVMK 680

Rattus norvegicus
Identities = 11/18 (61%)

Query 1 KDMQLGRLHMKTLLPVSK 18
K M LGR+ +K LLPV K
Sbjct 641 KGMLLGRIQIKALLPVMK 658

Eur. J. Immunol. 2002. 32: 2773–2782

The cleavage site of C5 from man and animals as a common target for neutralizing human monoclonal antibodies: *in vitro* and *in vivo* studies

Roberto Marzari[1], Daniele Sblattero[1], Paolo Macor[2], Fabio Fischetti[2], Renato Gennaro[3], James D. Marks[4], Andrew Bradbury[5,6] and Francesco Tedesco[2]

[1] Department of Biology, University of Trieste, Trieste, Italy
[2] Department of Physiology and Pathology, University of Trieste, Trieste, Italy
[3] Department of Biochemistry, Biophysics and Chemistry of Macromolecules (BBCM), University of Trieste, Trieste, Italy
[4] Department of Anesthesia, San Francisco General Hospital, San Francisco, USA
[5] Biosciences Division, Los Alamos National Laboratory, Los Alamos, USA
[6] SISSA, Trieste, Italy

The isolation of an anti-C5 single-chain fragment variable (scFv) antibody, TS-A12/22, from a human phage display library, is described. This antibody inhibits the activation of C5 and the assembly of the terminal complement complex implicated in cell and tissue damage. Using antibody-sensitized sheep erythrocytes and rabbit red cells as target cells in hemolytic assays, we found that TS-A12/22 inhibited the activation of C5 by the convertases of both classical and alternative pathways. Western blot analysis and competition experiments with synthetic peptides showed that TS-A12/22 reacted with the α chain of C5 and recognized the cleavage site of this complement component by the C5 convertase. As a result, the antibody prevented splitting of C5 and inhibited the generation of C5a and of the terminal complement complex. The identification of the TS-A12/22 recognition site as a conserved sequence in man, mouse, rat and rabbit enabled the demonstration of *in vitro* inhibition of complement activity in these species. The scFv TS-A12/22 was tested in a rat model of antigen-induced arthritis and proved to be effective in preventing influx of polymorphonuclear cells into the knee joint and C9 deposition on synovial tissue.

Key words: Complement / Inflammation / Single-chain fragment variable antibody / Phage display library

Received	18/4/02
Revised	11/6/02
Accepted	11/7/02

1 Introduction

The complement (C) system is an essential component of innate immunity and functions as a double-edged weapon ensuring on the one hand host protection and yet causing on the other hand tissue injury in several pathological conditions. The defensive functions are accomplished by biologically active products generated in the course of C activation, which opsonize infectious agents, promote inflammation or lyse susceptible targets. Unfortunately, these products, once released, do not differentiate between foreign and self targets and often cause extensive damage of bystander cells and tissues in clinical conditions associated with unrestricted C activation.

C5a and terminal C complex (TCC) are two of the C activation products that have been implicated in the promotion of tissue damage in several inflammatory diseases. Increased amounts of these products have been detected in the tissue fluids from patients with chronic inflammatory disorders, including rheumatoid arthritis and diseases of the central nervous system [1–4]. Elevated levels of C5a have also been found in the plasma of patients with multiple organ failure and myocardial ischemia-reperfusion injury, and the signs of pulmonary distress, hypotension and leukopenia usually seen in these patients are also observed in animals receiving intravenous administration of this anaphylatoxin [5]. C5a is also able to induce marked inflammatory reaction of the lung following intratracheal instillation into rabbits [6].

[I 23058]

Abbreviations: GVBS: Glucose veronal-buffered saline **MAC:** Membrane attack complex **C:** Complement **TCC:** Terminal C complex **scFv:** Single-chain fragment variable **C5D:** C5-deficient (human serum) **MPBS:** PBS containing 2% non-fat milk **mBSA:** Methylated BSA

0014-2980/02/1010-2773$17.50+.50/0

In recent years TCC has received special attention as one of the C activation products that may cause tissue injury because of non-lytic effects on phagocytes and endothelial cells leading eventually to inflammation [7, 8]. The complex has been localized in various tissues in several pathological conditions including rheumatoid arthritis, nephropathies, disorders of the central and peripheral nervous system and vascular diseases [9].

Given the critical role played by C5a and TCC in promoting chronic inflammation and tissue damage, many efforts have been made in recent years to neutralize the late components as a therapeutic measure in order to prevent the development of these complications in diseases associated with C activation. C5 is the ideal target of this strategy since neutralization of this C component will inhibit the activation of the terminal sequence without interfering with the opsonizing activity of the early components. Monoclonal antibodies to human [10, 11], mouse [12] and rat [13] C5 have been developed that inhibit generation of C5a and membrane attack complex (MAC). Antibodies to C5 have been successfully used in mice to prevent the development of collagen-induced arthritis [14] and to improve the clinical course of glomerulonephritis [15], and in rats to reduce myocardial ischemia and reperfusion [13].

In the last few years two anti-human C5 single-chain fragment variable (scFv) have been constructed that show more rapid tissue penetration compared to whole antibodies. The first is a murine scFv obtained by assembling the variable regions of a murine mAb to C5 [16]. This retained the ability of the original mAb to inhibit the assembly of MAC and partially blocked C5a generation. This antibody was also shown to prevent deposition of C5b–9 in mouse heart perfused with human plasma and also in heart failure. The second scFv is a humanized murine mAb to human C5 that was obtained by grafting the complementarity-determining regions into human heavy and light variable region frameworks. This is able to prevent generation of both C5a and C5b–9, although the epitope recognized by this antibody and its localization on the C5 molecule has not been reported [17]. More recently, Fitch et al. [18] have published data indicating that this scFv administered to a group of patients with cardiopulmonary bypass at a dose of 2 mg/ml totally inhibited C hemolytic activity for up to 14 h and attenuated myocardial damage, cognitive deficits and blood loss.

In this study we report an scFv against human C5 isolated from a large naive antibody library that was derived from rearranged V genes amplified from peripheral blood lymphocytes of unimmunized human donors. The novelty of this scFv is that it reacts with an epitope localized on the α chain of human C5 at the site of cleavage of the molecule into C5a and C5b and is also effective in inhibiting the activation of C5 from other animals including rat, rabbit and mouse. Evidence indicating that the anti-C5 scFv prevents antigen-induced arthritis and tissue deposition of C9 is also provided.

2 Results

2.1 Identification and characterization of an anti-C5 clone that blocks the cleavage of C5

Twelve positive clones, TS-A1 to 12, expressing antibodies directed against human C5 were isolated and processed to prepare soluble periplasmic scFv, which were then used to further select clones that inhibited the activation of C5, as evaluated by the amount of C5a and TCC released in the supernatant. One of these clones, TS-A12, inhibited the generation of both C5a and TCC (Fig. 1) and was specific for C5 because it did not react with either C3 or C4 or with the other terminal components, as determined by ELISA (data not shown). Since the equilibrium dissociation constant (K_d) of TS-A12 was 2×10^{-7} M, VL chain shuffling was performed to increase its affinity. Five clones reactive with C5 were generated; and one of these, TS-A12/22, shared with the parental clone the ability to inhibit the cleavage of C5, but exhibited a tenfold higher affinity with a value of 1.8×10^{-8} M. The VH gene of the two clones derived from VH3/V-48 gene family/segment, while the VL gene derived from Vλ3/V2–14 and Vκ4/DPK24 for TS-A12 and TS-A12/22, respectively. All subsequent studies were performed on TS-A12/22.

2.2 Definition of the target specificity of TS-A12/22

To search for the site of action of TS-A12/22, we tested the reactivity of this scFv with purified C5α and C5β subunits by SDS-PAGE and immunoblotting. Fig. 2 shows that TS-A12/22 selectively interacts with C5α, suggesting that it may recognize an epitope localized on the cleavage site of the C5 convertase. To confirm this, we incubated TS-A12/22 with the P5A-18 peptide prior to addition of the mixture to bound C5 in a competitive ELISA and observed a dose-dependent inhibition of anti-C5 scFv binding to C5, while both an unrelated peptide and C5a were ineffective even at the highest concentration (Fig. 3).

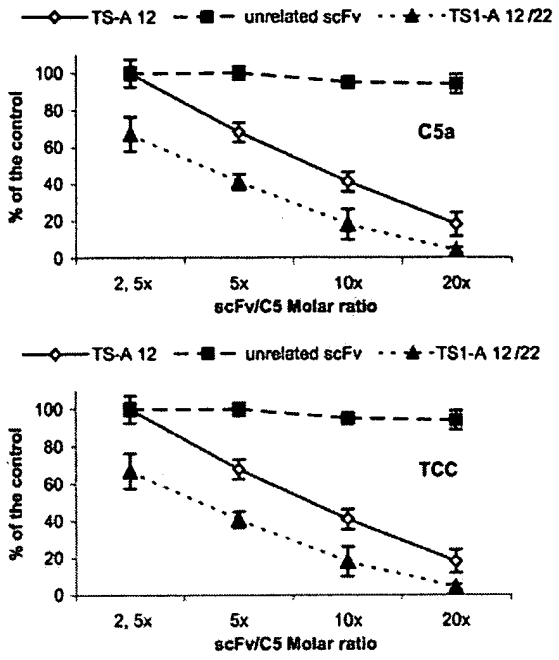

Fig. 1. Evaluation of C5a and TCC formed as a result of C5 activation in the presence of TS-A12, TS-A12/22 and unrelated scFv. The results obtained at different scFv/C5 molar ratios are expressed as mean ± SD of percent value of the control (GVBS) in three different experiments.

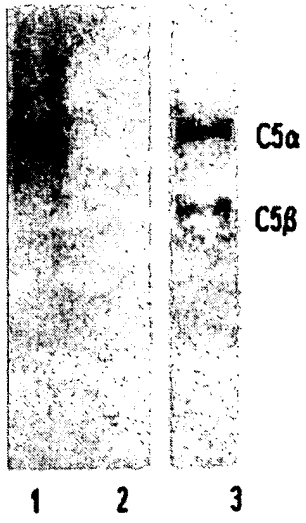

Fig. 2. Immunoblot analysis of purified C5 α and β chains using 100 ng of each subunit and TS-A12/22 as revealing scFv. Lane 1: C5α; lane 2: C5β; lane 3: mixture of the two chains. The immunoblot was developed with 1/500 TS-A12/22 followed by 1/1,000 mAb anti-SV5 and 1/1,000 alkaline phosphatase-labeled goat anti-mouse IgG. Lane 3 was developed with 1/1,000 biotin-labeled goat anti-human C5 followed by 1/4,000 streptavidin-alkaline phosphatase.

2.3 Functional characterization of TS-A12/22

Having found that TS-A12/22 blocks the cleavage of C5, we addressed the issue whether this scFv is able to inhibit the activation of C5 by both the classical and the alternative pathway of C activation. The results presented in Fig. 4 show that TS-A12/22 inhibited C5-dependent lysis triggered through both pathways to a similar extent. We also tested TS-A12/22 for its ability to inhibit the hemolytic activity of C5 from various animals, and found that the anti-C5 scFv was effective on C5 from rabbit, rat and mouse sera, although the amount of sera required to obtain similar hemolytic activity varied between these species (Fig. 5).

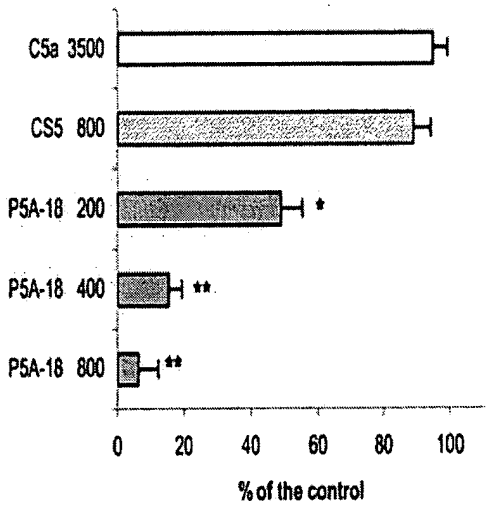

Fig. 3. Inhibition of TS-A12/22 binding to C5 by C5 (P5A-18) and fibronectin (CS5) peptides. Mixtures of TS-A12/22 (1 μg/ml) and various concentrations of peptides to a final volume of 100 μl were incubated for 15 min at room temperature and then added to bound C5 (250 ng). Binding of TS-A12/22 to C5 was evaluated as described Sect. 4. Data are presented as mean ± SD of percent value of the control (GVBS) obtained in three different experiments. *$p<0.05$ and **$p<0.01$ versus control.

2.4 TS-A12/22 prevents joint inflammation in antigen-induced arthritis

To evaluate the *in vivo* effect of TS-A12/22, we measured the influx of PMN into the joints of rats that have received an intraarticular injection of anti-C5 scFv and methylated BSA (mBSA), and compared the results with those obtained with mBSA alone or with mBSA mixed with an unrelated scFv. Fig. 6 shows that the number of PMN induced to migrate into the knee by mBSA remained

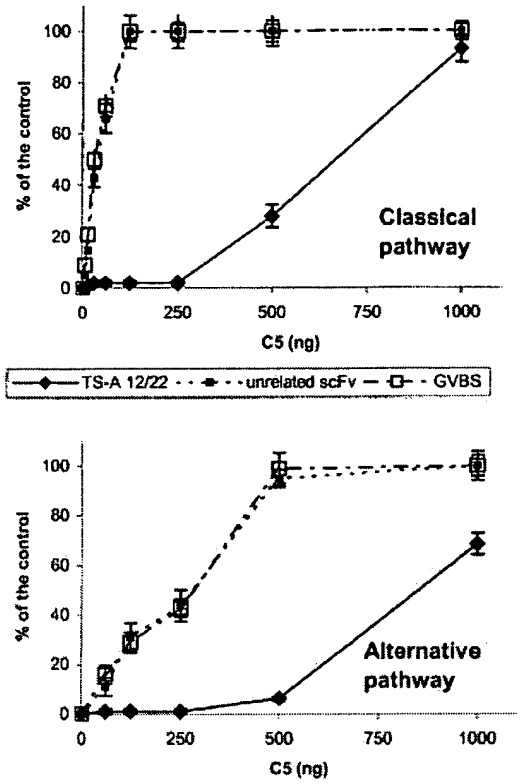

Fig. 4. Inhibition of C5 hemolytic activity by TS-A12/22. Increasing amounts of C5 were mixed with either TS-A12/22 (600 ng) or an unrelated scFv (600 ng) or GVBS and incubated for 15 min at room temperature prior to addition to 50 μl of the appropriate target erythrocytes. Data are presented as mean ± SD of percent value obtained in three different experiments.

essentially unchanged in rats receiving an unrelated scFv but dropped to a negligible level in rats treated with the anti-C5 scFv. In addition, injection of TS-A12/22 did not reduce the synovial deposition of C3, but blocked almost completely that of C9 (Fig. 7).

3 Discussion

Efforts are being made by several groups to develop pharmacological agents capable of neutralizing the undesired effects of C activation in chronic clinical conditions using either competing peptides or blocking antibodies [19]. An ideal reagent should be effective in blocking the damaging effects of C activation products without affecting the protective functions of the system. This consideration led us to select C5 as a potential target of neutralizing antibodies since its activation products have been implicated in tissue destruction in many pathological conditions. A complete inhibition of all C activation pathways can also be obtained by blocking C3, but the risk of long-term depletion of C3 is the frequent occurrence of serious infections sustained by encapsulated bacteria and fungi, whereas C5-deficient patients usually suffer from short self-limiting neisserial infections. While choosing C5 as an ideal target to deplete, it was important for us to establish that the antibodies used in the present study were specific for C5 and were able to selectively neutralize its functional activity. The results of ELISA excluded any cross-reaction of our anti-C5 antibodies with other C components, especially with C3 and C4, which belong to the same protein family as C5 [20].

An important requirement for antibodies intended for clinical application is that they are not immunogenic, particularly if considered for long-term use. In general, such reagents have been generated by immunization of mice, with selection of monoclonal antibodies with the desired properties. The major problem associated with this approach is that murine antibodies are generated, with the attendant risk of generating an immune response when used in therapy. This problem can be partially overcome by cloning the V regions and 'humanizing' them [21, 22], as has been reported for the production of a humanized anti-C5 antibody [16]. In this procedure, amino acids characteristic of the murine framework and thus likely to induce an immune response, are exchanged for their human counterparts. This approach has been used successfully for the production of several humanized antibodies including herceptin, an anti-c-ErbB2 antibody presently used for the treatment of breast cancer, rituximab, an anti-CD20 antibody found to be efficacious against follicular non-Hodgkin lymphoma, and infliximab, an anti-TNF antibody used for treatment of rheumatoid arthritis and Crohn's disease [23]. Although humanized antibodies are thought to be minimally immunogenic when administered to man, an anti-globulin response may still be a problem particularly in patients who receive repeated administrations of these antibodies [24]. We have followed the alternative approach of using a phage display library obtained from human lymphocytes to prepare anti-C5 scFv antibodies.

TS-A12/22 antibodies proved to be effective in inhibiting the splitting of activated C5 into C5a and C5b. Evidence supporting this conclusion is based on our failure to detect measurable amounts of C5a and to induce MAC-dependent lysis of susceptible erythrocytes when C5 was activated by either the classical or alternative C pathways in the presence of TS-A12/22. Three murine monoclonal antibodies that bind to the β chain of C5 and block cleavage of human C5 inhibiting the generation of TCC and C5a have previously been reported by Wurzner et al. [10] and Wang et al. [11]. Our anti-C5 scFv differs

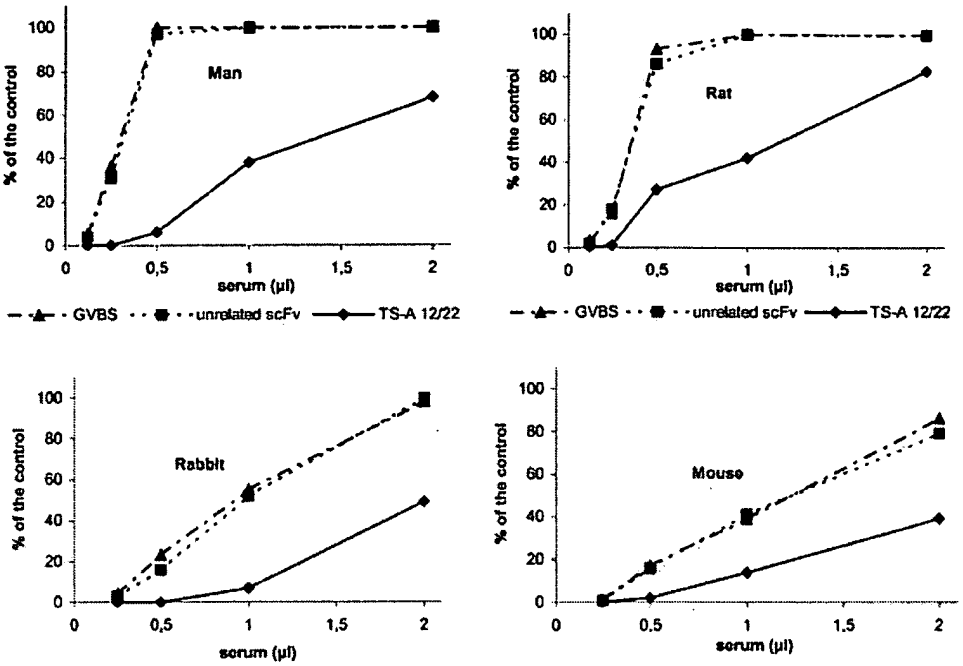

Fig. 5. Inhibition of hemolytic activity of C5 from various animals by TS-A12/22.The experimental conditions are similar to those reported in the legend to Fig. 4.

from these antibodies in that it reacts with the α chain of C5, as determined by Western blot analysis, and recognizes an epitope localized at the cleavage site of the C5 convertase. This was proved by the results of inhibition experiments showing that an 18-amino acid peptide encompassing the cleavage area inhibited binding of TS-A12/22 to C5, whereas C5a was totally ineffective. The reason for the inhibition of C5 splitting observed with antibodies reacting with the β chain is not apparent, but recent data obtained by Low and coworkers [25] using C5 mutants and synthetic peptides to inhibit C hemolytic activity suggest that sites of C5 distal to its cleavage area are involved in the interaction with the C5 convertases.

The only anti-C5 antibody tested in patients is the humanized h5G1.1 scFv, and its derivatives, which has been shown to inhibit *in vivo* generation of TCC and C-dependent hemolytic activity in patients undergoing cardiopulmonary bypass, although the epitope recognized by this antibody has not been reported [16, 17]. h5G1.1 does not seem to be effective on C5 derived from other animals and this precludes its use in animal models, which would be helpful in the evaluation of their *in vivo* effects prior to use in man. By contrast, TS-A12/22 is able to inhibit cleavage of C5 to C5a and C5b in at least three other species (mouse, rat and rabbit), indicating that this antibody can be extensively validated in preclinical models in a fashion which is not possible with other available antibodies. The different behavior of h5G1.1 and TS-A12/22 may be related to the fact that the epitope located at the cleavage site and recognized by TS-

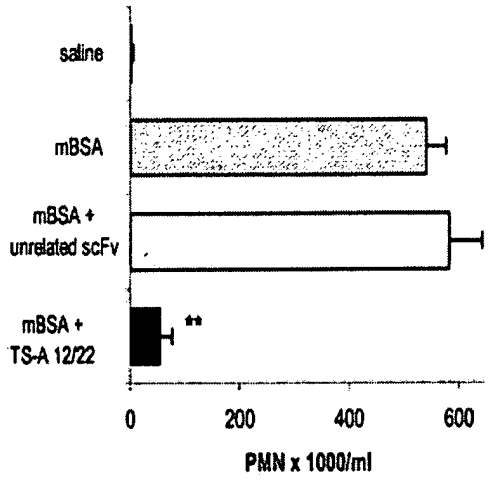

Fig. 6. Number of PMN in the lavage of rat joints collected 36 h after injection of saline or mixtures of mBSA and either TS-A12/22 or unrelated scFv. The results are presented as mean cell number ± SD obtained in three different experiments. $^{**}p<0.01$ versus mBSA.

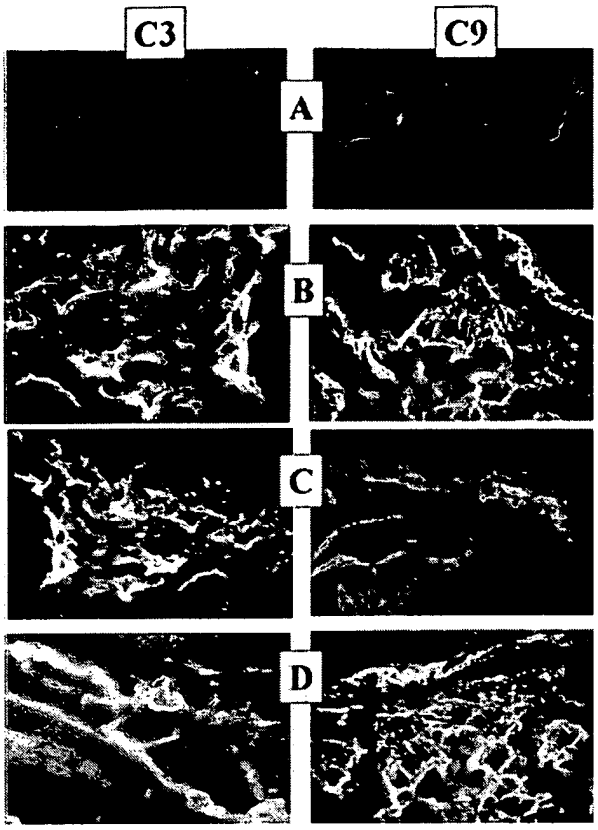

Fig. 7. Immunofluorescence analysis of synovial membranes obtained from rats receiving intraarticular injection of saline (A), mBSA (B), mBSA and TS-A12/22 (C), mBSA and unrelated scFv (D) for deposition of C3 and C9.

A12/22 is highly conserved between mouse and man. Antibodies, such as h5G1.1, obtained by immunization, are constrained by the limits of the immune system of the animal used for immunization. In particular, it tends to be very difficult to derive antibodies against conserved antigens by immunization. Since tolerance against self epitopes is mediated at the level of specific VH/VL combinations, the creation of novel VH/VL combinations, as occurs in phage antibody libraries [26], results in the suspension of these immunological constraints and the ability to select antibodies against self antigens [27].

The recognition of the exact site of cleavage of C5 by C5 convertase, by either the classical or alternate pathway, represents a powerful tool in the therapeutic manipulation of the C system. The potential clinical usefulness of a reagent with this specificity is underscored by the inhibition of intraarticular migration of PMN and of C9 deposition on synovial tissue in an experimental model of antigen-induced arthritis. Pathological processes in which this antibody would be expected to be useful include all those involving acute or chronic inflammation, such as rheumatoid arthritis [28], and ischemia reperfusion following myocardial infarction [13].

VL chain shuffling proved useful to increase the affinity of TS-A12 initially selected from the antibody library. This highlights another advantage of the use of phage display to generate antibodies: in addition to the derivation of anti-self specificities, antibodies, once selected, can have their affinities matured by combinations of chain shuffling [29] and parsimonious mutagenesis [30], to picomolar levels rarely achieved by immunization.

In conclusion we have identified and characterized a human scFv anti-human C5 antibody, which inhibits the activation of C5 and blocks the generation of its activation products. This antibody may be used for treatment of inflammatory processes after an appropriate evaluation of its efficacy in animal models.

4 Materials and methods

4.1 Sera and C reagents

Human C5-deficient (C5D) serum was obtained from a patient with a history of meningococcal disease identified in our laboratory because of undetectable level of C5 and lack of hemolytic activity, which was reconstituted by purified C5. Sera were also obtained from blood donors, New Zealand rabbits, Wistar rats and CBA mice and used as a source of C. Purified C components from C4 to C9 were purchased from Quidel (San Diego, CA) and recombinant human C5a was supplied from Sigma-Aldrich (Milan, Italy). C5α and β subunits were obtained by incubating 50 μg C5 diluted in 0.55 M Tris-HCl pH 8.1 with 0.02 M dithiothreitol for 30 min at room temperature followed by treatment with 0.12 M iodoacetamide for 1 h at room temperature. The two chains were purified by fast protein liquid chromatography (FPLC) on Superose 12 (Pharmacia Biotech, Milan, Italy) and checked for purity by SDS-PAGE under nonreducing conditions.

4.2 Antisera

Two anti-human C5a mAb, G25/2 and C17/5, the latter recognizing a neoepitope exposed on this fragment, were a kind gift from Prof. O. Götze (Göttingen, Germany). mAb aE11 directed against a C9 neoantigen was kindly provided by Prof. T. Lea (Oslo, Norway). Goat antiserum to C5 was purchased from Quidel and alkaline phosphatase-labeled goat anti-mouse IgG from Sigma-Aldrich. Rabbit antiserum to rat C9 was obtained through the courtesy of Prof. P. Morgan (Cardiff, GB) and anti-SV5 mAb recognizing the SV5 tag at the scFv C terminus was a gift from Dr. Randall (St. Andrews, GB). Purification of IgG by affinity chromatography

on protein G and biotin labeling of antibodies and C5 were performed following published procedure [31].

4.3 Library and bacteria

The antibody library used has been previously described [32] and has a diversity of 7.0×10^9 derived from nonimmune peripheral blood lymphocytes. *Escherichia coli* DH5aF' strain was used for phage propagation and HB2151 strain was used to make soluble scFv.

4.4 Rescue of phagemid library and panning

Phagemid particles were rescued as previously described [33]. Panning was performed in immunotubes (Nunc, Mascia Brunelli, Milan, Italy) coated with purified C5, 10 μg/ml in PBS, overnight at 4°C as previously reported [34]. The panning procedure was repeated up to three times. After the second cycle, the eluting *E. coli* cells were grown and the phagemid DNA was extracted by conventional methods. The phagemid DNA was used as a template for VH and VL individual PCR amplifications, assembly and cloning into pDAN5 [35], a newly developed phagemid vector improved by insertions of lox sequences, His_6 and SV5 [36] tags, and characterized by inversion of the order VH and VL sequences. After transformation, the *E. coli* cells were rescued by helper phage and the phage particles used for the third panning.

4.5 Evaluation of antibody specificity of phage clones

After panning, individual clones were screened for antigen reactivity. Phages from individual colonies were grown in 96-well plates. ELISA were performed in microtiter plates coated with the antigen (10 μg/ml) by overnight incubation in 0.1 M sodium bicarbonate buffer pH 9.6 at 4°C. After saturation with PBS containing 2% non-fat milk (MPBS), 50 μl phage suspension diluted with an equal volume of MPBS and mAb anti-phage gene 3 protein conjugated with horseradish peroxidase (Pharmacia Biotech) were sequentially added. Binding was revealed using H_2O_2 and 3,3',5,5'-tetramethylbenzidine dihydrochloride (Sigma-Aldrich) as substrate and read at 450 nm.

4.6 Fingerprinting and sequencing of the clones

The V genes of positive clones for each protein were amplified by PCR using V gene primers as described [33]. The V genes from the different anti-C5 scFv clones were sequenced, and the VH and VL families as well as the gene segments used were assessed by screening against the VBASE (http://www.mrc-cpe.cam.ac.uk/imt-doc/restricted/ok.html) database [37].

4.7 Preparation of soluble scFv

Phages from individual colonies were used to infect HB2151 bacteria grown as previously described [34]. The periplasmic scFv fraction was prepared by extraction of pelleted bacteria with B-PER reagent (Pierce, Celbio, Milan, Italy) for 20 min at room temperature followed by centrifugation for 15 min at 27,000×g. The supernatant was collected and dialyzed against PBS. Purified scFv were obtained by affinity chromatography of the bacterial extract on Ni-NTA resin (Qiagen, Milan, Italy), which selectively binds the six histidines at the C terminus of the scFv.

4.8 Measurement of binding by surface plasmon resonance

Affinity measurements were conducted in a BIACORE 2000 system (Biacore AB, Uppsala, Sweden). Purified C5 (20 μg/ml in 10 mM sodium acetate pH 4.5) was coupled to a sensor chip CM5 (~1,000 RU) by direct coupling to primary amines, and the subsequent measures carried out as described in [38]. Equilibrium constant was calculated as $K_d=K_{on}/K_{off}$.

4.9 Antibody chain shuffling

VL chain shuffling [39] of scFv TSA-12 was carried out as follows: phagemid DNA was digested with BssHII and SalI to excise the VL region. The replacement of the VL gene was obtained using the repertoire of VL chains obtained by cutting a preimmune human library [35] with the same enzymes. After ligation and cloning, a library of nearly 10^6 clones was obtained. The library underwent three rounds of selection on biotin-labeled C5, as described by Hawkins et al. [40].

4.10 Evaluation of scFv binding to C5

An ELISA was used to measure the binding of scFv antibodies to C5. Wells of microtiter plates were coated with purified C5 (250 ng) by overnight incubation in 0.1 M sodium bicarbonate buffer pH 9.6 at 4°C. After washing with PBS containing 0.1% Tween 20, the residual free binding sites were blocked with MPBS for 1 h at 37°C. The bound C5 was allowed to react either with a dilution of the bacterial extracts or with purified scFv (1 μg/ml) followed by 1/1,000 mAb anti-SV5 and 1/1,000 alkaline phosphatase-labeled goat anti-mouse IgG (Sigma-Aldrich). All these steps were carried out for 1 h at 37°C. The enzymatic reaction was developed using p-nitrophenyl phosphate (1 mg/ml; Sigma-Aldrich) as a substrate in 0.1 M glycine buffer pH 10.4 containing 1 mM $MgCl_2$ and 1 mM $ZnCl_2$, and read at 405 nm using a Titertek Multiskan ELISA reader (Flow Labs, Milan, Italy).

4.11 Peptide synthesis and purification

The peptide corresponding to residues 727–744 of human C5 (KDMQLGRLHMKTLLPVSK; [41]) was synthesized as a C-terminal amide by the solid phase method, using the 9-fluorenylmethoxycarbonyl (Fmoc) chemistry. For each coupling step, the Fmoc-protected amino acid and coupling reagents (TBTU and HOBt) were added in a six- to eightfold molar excess with respect to resin substitution. The peptide was cleaved and deprotected with trifluoroacetic acid, water, triisopropylsilane and 1,2-ethanedithiol (92.5:3.0:2.0:2.5 vol/vol) and purified by reverse phase-HPLC on a C18 column, using a 0–60% water/acetonitrile gradient in 0.1% trifluoracetic acid. Peptide concentration was determined by the method of Waddell [42], and its molecular mass was determined with an electrospray mass spectrometer. The CS5 fragment of fibronectin (GEEIQIGHIPREDVDYHLYP) was used as an unrelated peptide control.

4.12 Erythrocyte intermediates and hemolytic assays

SRBC were sensitized with subagglutinating amount of rabbit IgM antibodies. The intermediate Ab-sensitized SRBC bearing classical C5 convertase (EAC1–3b) were prepared by incubating sensitized SRBC with 1/10 C5D serum in glucose veronal-buffered saline (GVBS) for 70 s at 37°C followed by the addition of suramin (Bayer, Germany) to block the reaction [43]. C alternative pathway was activated by suspending rabbit erythrocytes in 1/10 C5D serum diluted in GVBS containing 10 mM EGTA and 5 mM $MgCl_2$. The lytic assays were performed by incubating 50 µl of the appropriate erythrocytes (1.5×10^7) in 200 µl of GVBS containing the source of C reagents for 30 min at 37°C, and then reading the supernatant after centrifugation at 415 nm.

4.13 Quantitation of C5a and TCC

A mixture containing 50 µl of 1% EAC1–3b, 100 µl of 1:100 C5D serum and 50 ng of C5 to a final volume of 250 µl using GVBS as diluent was incubated for 30 min at 37°C. The red cells were then removed by centrifugation at 4°C and the supernatant was collected for the quantitation of C5a and TCC. The level of C5a was measured using mAb C17/5 as trapping antibody and mAb G25/2 as revealing reagent according to Oppermann et al. [44]. The amount of TCC was evaluated using solid phase-bound mAb aE11 and biotin-labeled goat IgG anti-C5 followed by alkaline phosphatase conjugate to streptavidin (Sigma-Aldrich) following published procedure [45].

4.14 SDS-PAGE and immunoblotting

The α and β chains of C5 were analyzed by SDS-PAGE on a 10% gel under nonreducing conditions and transferred electrophoretically onto nitrocellulose membrane (Hybond ECL, Amersham, Milan, Italy). The interaction of membrane-bound C5 subunits with TS-A12/22 or biotin-labeled goat anti-C5 followed by alkaline phosphatase-conjugated secondary antibody or by alkaline phosphatase-labeled streptavidin (Sigma-Aldrich) was performed according to published procedure [31].

4.15 Induction of arthritis and disease assessment

Antigen-induced arthritis was established in 12 female Wistar rats weighing 240–270 g following two intradermal injections at the base of the tail of an emulsion containing equal volumes of 100 mg mBSA in 200 ml of sterile saline and Freund's complete adjuvant, both from Sigma-Aldrich, on days 0 and 7. Fourteen days after the second injection, arthritis was induced by intraarticular administration of mBSA (100 mg in 100 ml of saline) into the right knee of each animal, while saline was injected as a vehicle into the left knee and served as a control. One group of four animals was treated with mBSA alone, while two other groups of four animals each received a mixture of 100 mg of mBSA and 400 mg of either anti-C5 or anti-gliadin scFv.

The rats were killed 36 h after intraarticular treatment and the knee joints were washed with 1 ml of saline solution. The total number of cells in the joint lavage was measured by a ZBI Coulter Counter (Coulter Electronics, Luton, GB) and that of PMN was assessed by measuring the myeloperoxidase content in an assay system containing 0.05% cetyltrimetylammonium bromide, 2 mM 3-amino-11,2,4-triazole, 1 mM tetramethylbenzidine, all purchased from Sigma-Aldrich, and 0.35 mM H_2O_2 at 450 nm [46]. Frozen sections were analyzed for tissue deposition of C3 following incubation with 1:200 goat anti-C3 antibody (Cappel, ICN Pharmaceutical, DBA, Milan, Italy) for 60 min at room temperature and further exposure to 1/200 FITC-labeled rabbit $F(ab')_2$ anti-goat IgG (Southern Biotechnology Associates, Birmingham, AL) for additional 60 min at room temperature. A similar approach was followed to examine the synovial tissue for the presence of C9 except that 1:1,000 IgG rabbit anti-rat C9 was used followed by 1:400 biotin-labeled goat anti-rabbit IgG (Sigma-Aldrich) and 1/50 FITC-labeled streptavidin (DAKO S.p.A., Milan, Italy).

4.16 Statistical analysis

The results are expressed as means ± SD. Statistical significance was determined using the Student's *t*-test to compare two groups of data.

Acknowledgements: We are grateful to G. Scatassa and C. Rigo for excellent technical assistance. This work was supported by grants provided by the Italian MIUR (60% and Cofin), CNR (Target project on Biotechnology), Ministry of

Health (Progetto Finalizzato Cod. B08), EU-concerted action (contract no. QLG1-CT-2001-01039) and Regione Friuli-Venezia Giulia.

References

1 **Jose, P. J., Moss, I. K., Maini, R. N. and Williams, T. J.,** Measurement of the chemotactic complement fragment C5a in rheumatoid synovial fluids by radioimmunoassay: role of C5a in the acute inflammatory phase. *Ann. Rheum. Dis.* 1990. **49:** 747–752.

2 **Mollnes, T. E., Lea, T., Mellbye, O. J., Pahle, J., Grand, O. and Harboe, M.,** Complement activation in rheumatoid arthritis evaluated by C3dg and the terminal complement complex. *Arthritis Rheum.* 1986. **29:** 715–721.

3 **Hartung, H. P., Schwenke, C., Bitter-Suermann, D. and Toyka, K. V.,** Guillain-Barre syndrome: activated complement components C3a and C5a in CSF. *Neurology* 1987. **37:** 1006–1009.

4 **Sanders, M. E., Alexander, E. L., Koski, C. L., Shin, M. L., Sano, Y., Frank, M. M. and Joiner, K. A.,** Terminal complement complexes (SC5b–9) in cerebrospinal fluid in autoimmune nervous system diseases. *Ann. N.Y. Acad. Sci.* 1988. **540:** 387–388.

5 **Ember, J. A., Jagels, M. A. and Hugli, T. E.,** Characterization of complement anaphylatoxins and their biological responses. In **Volanakis, J. E. and Frank, M. M. (Eds.)** *The human complement system in health and disease.* Marcel Dekker, New York 1998, pp 241–284.

6 **Larsen, G. L., McCarthy, K., Webster, R. O., Henson, J. and Henson, P. M.,** A differential effect of C5a and C5a des Arg in the induction of pulmonary inflammation. *Am. J. Pathol.* 1980. **100:** 179–192.

7 **Morgan, B. P,** Complement membrane attack on nucleated cells: resistance, recovery and non-lethal effects. *Biochem. J.* 1989. **264:** 1–14.

8 **Tedesco, F., Fischetti, F., Pausa, M., Dobrina, A., Sim, R. B. and Daha, M. R.,** Complement-endothelial interactions: pathophysiological implications. *Mol. Immunol.* 1999. **36:** 261–268.

9 **Hänsch, G. M. and Shin, M.,** Complement attack phase. In **Rother, K., Till, G. O. and Hänsch, G. M. (Eds.)** *The complement system.* Springer, Berlin 1998, p 115.

10 **Würzner, R., Schulze, M., Happe, L., Franzke, A., Bieber, F. A., Oppermann, M. and Götze, O.,** Inhibition of terminal complement complex formation and cell lysis by monoclonal antibodies. *Complement Inflamm.* 1991. **8:** 328–340.

11 **Wang, X., Sahu, A., Pangburn, M. K. and Wetsel, R. A.,** Inhibition of C5 cleavage but not C5 binding by a monoclonal antibody that recognizes an 85 amino acid region of C5 β chain. *Mol. Immunol.* 1996. **33:** 56.

12 **Frei, Y., Lambris, J. D. and Stockinger, B.,** Generation of a monoclonal antibody to mouse C5. Application in an ELISA assay for detection of anti-C5 antibodies. *Mol. Cell Probes* 1987. **1:** 141–149.

13 **Vakeva, A. P., Agah, A., Rollins, S. A., Matis, L. A., Li, L. and Stahl, G. L.,** Myocardial infarction and apoptosis after myocardial ischemia and reperfusion: role of the terminal complement components and inhibition by anti-C5 therapy. *Circulation* 1998. **97:** 2259–2267.

14 **Wang, Y., Rollins, S. A., Madri, J. A. and Matis, L. A.,** Anti-C5 monoclonal antibody therapy prevents collagen-induced arthritis and ameliorates established disease. *Proc. Natl. Acad. Sci. USA* 1995. **92:** 8955–8959.

15 **Wang, Y., Hu, Q., Madri, J. A., Rollins, S. A., Chodera, A. and Matis, L. A.,** Amelioration of lupus-like autoimmune disease in NZB/WF1 mice after treatment with a blocking monoclonal antibody specific for complement component C5. *Proc. Natl. Acad. Sci. USA* 1996. **93:** 8563–8568.

16 **Evans, M. J., Rollins, S. A., Wolff, D. W., Rother, R. P., Norin, A. J., Therrien, D. M., Grijalva, G. A., Mueller, J. P., Nye, S. H., Squinto, S. P. and Wilkins, J. A.,** In vitro and in vivo inhibition of complement activity by a single-chain Fv fragment recognizing human C5. *Mol. Immunol.* 1995. **32:** 1183–1195.

17 **Thomas, T. C., Rollins, S. A., Rother, R. P., Giannoni, M. A., Hartman, S. L., Elliott, E. A., Nye, S. H., Matis, L. A., Squinto, S. P. and Evans, M. J.,** Inhibition of complement activity by humanized anti-C5 antibody and single-chain Fv. *Mol. Immunol.* 1996. **33:** 1389–1401.

18 **Fitch, J. C., Rollins, S., Matis, L., Alford, B., Aranki, S., Collard, C. D., Dewar, M., Elefteriades, J., Hines, R., Kopf, G., Kraker, P., Li, L., O'Hara, R., Rinder, C., Rinder, H., Shaw, R., Smith, B., Stahl, G. and Shernan, S. K.,** Pharmacology and biological efficacy of a recombinant, humanized, single-chain antibody C5 complement inhibitor in patients undergoing coronary artery bypass graft surgery with cardiopulmonary bypass. *Circulation* 1999. **100:** 2499–2506.

19 **Sahu, A. and Lambris, J. D.,** Complement inhibitors: a resurgent concept in anti-inflammatory therapeutics. *Immunopharmacology* 2000. **49:** 133–148.

20 **Sottrup-Jensen, L., Stepanik, T. M., Kristensen, T., et al.,** Common evolutionary origin of alpha 2-macroglobulin and complement components C3 and C4. *Proc. Natl. Acad. Sci. USA* 1985. **82:** 9–13.

21 **Gussow, D. and Seemann, G.,** Humanization of monoclonal antibodies. *Methods Enzymol.* 1991. **203:** 99–121.

22 **Kettleborough, C. A., Saldanha, J., Heath, V. J., Morrison, C. J. and Bendig, M. M.,** Humanization of a mouse monoclonal antibody by CDR-grafting: the importance of framework residues on loop conformation. *Protein Eng.* 1991. **4:** 773–783.

23 **Breedveld, F. C.,** Therapeutic monoclonal antibodies. *Lancet.* 2000. **355:** 735–743.

24 **Isaacs, J. D., Watts, R. A., Hazleman, B. L., Hale, G., Keogan, M. T., Cobbold, S. P. and Waldmann, H.,** Humanised monoclonal antibody therapy for rheumatoid arthritis. *Lancet* 1992. **340:** 748–752.

25 **Low, P. J., Ai, R. and Ogata, R. T.,** Active sites in complement components C5 and C3 identified by proximity to indels in the C3/4/5 protein family. *J. Immunol.* 1999. **162:** 6580–6588.

26 **Clackson, T., Hoogenboom, H. R., Griffiths, A. D. and Winter, G.,** Making antibody fragments using phage display libraries. *Nature* 1991. **352:** 624–628.

27 **Griffiths, A. D., Malmqvist, M., Marks, J. D., et al.,** Human anti-self antibodies with high specificity from phage display libraries. *EMBO J.* 1993. **12:** 725–734.

28 **Matsumoto, I., Maccioni, M., Lee, D. M., Maurice, M., Simmons, B., Brenner, M., Mathis, D. and Benoist, C.,** How antibodies to a ubiquitous cytoplasmic enzyme may provoke joint-specific autoimmune disease. *Nat. Immunol.* 2002. **3:** 360–365.

29 **Marks, J. D., Hoogenboom, H. R., Griffiths, A. D. and Winter, G.,** Molecular evolution of proteins on filamentous phage. Mimicking the strategy of the immune system. *J. Biol. Chem.* 1992. **267:** 16007–16010.

30 **Schier, R., Balint, R. F., McCall, A., Apell, G., Larrick, J. W. and Marks, J. D.,** Identification of functional and structural amino-acid residues by parsimonious mutagenesis. *Gene* 1996. **169:** 147–155.

31 **Langeggen, H., Pausa, M., Johnson, E., Casarsa, C., and Tedesco, F.,** The endothelium is an extrahepatic site of synthesis of the seventh component of the complement system. *Clin. Exp. Immunol.* 2000. **121:** 69–76.

32 **Sheets, M. D., Amersdorfer, P., Finnern, R., Sargent, P., Lindquist, E., Schier, R., Hemingsen, G., Wong, C., Gerhart, J. C., Marks, J. D. and Lindqvist, E.,** Efficient construction of a large nonimmune phage antibody library: the production of high-affinity human single-chain antibodies to protein antigens. *Proc. Natl. Acad. Sci. USA* 1998. **95:** 6157–6162.

33 **Marks, J. D., Hoogenboom, H. R., Bonnert, T. P., McCafferty, J., Griffiths, A. D. and Winter, G.,** By-passing immunization. Human antibodies from V-gene libraries displayed on phage. *J. Mol. Biol.* 1991. **222:** 581–597.

34 **Marzari, R., Sblattero, D., Florian, F., Tongiorgi, E., Not, T., Tommasini, A., Ventura, A. and Bradbury, A.,** Molecular dissection of the tissue transglutaminase autoantibody response in celiac disease. *J Immunol.* 2001. **166:** 4170–4176.

35 **Sblattero, D. and Bradbury, A.,** Exploiting recombination in single bacteria to make large phage antibody libraries. *Nat. Biotechnol.* 2000. **18:** 75–80.

36 **Hanke, T., Szawlowski, P. and Randall, R. E.,** Construction of solid matrix-antibody-antigen complexes containing simian immunodeficiency virus p27 using tag-specific monoclonal antibody and tag-linked antigen. *J. Gen. Virol.* 1992. **73:** 653–660.

37 **Tomlinson, I. M., Williams, S. C., Corbett, S. J., Cox, J. P. L. and Winter, G.,** BASE sequence directory. MRC Centre for Protein Engineering, Cambridge 1996.

38 **Cirino, N. M., Sblattero, D., Allen, D., Peterson, S. R., Marks, J. D., Jackson, P. J., Bradbury, A. and Lehnert, B. E.,** Disruption of anthrax toxin binding with the use of human antibodies and competitive inhibitors. *Infect. Immun.* 1999. **67:** 2957–2963.

39 **Schier, R., Bye, J., Apell, G., McCall, A., Adams, G. P., Malmqvist, M., Weiner, L. M. and Marks, J. D.,** Isolation of high-affinity monomeric human anti-c-erbB-2 single chain Fv using affinity-driven selection. *J. Mol. Biol.* 1996. **255:** 28–43.

40 **Hawkins, R. E., Russell, S. J. and Winter, G.,** Selection of phage antibodies by binding affinity. Mimicking affinity maturation. *J. Mol. Biol.* 1992. **226:** 889–896.

41 **Haviland, D. L., Haviland, J. C., Fleischer, D. T., Hunt, A. and Wetsel, R. A.,** Complete cDNA sequence of human complement pro-C5. Evidence of truncated transcripts derived from a single copy gene. *J. Immunol.* 1991. **146:** 362–368.

42 **Waddell, W. J.,** A simple ultraviolet spectrophotometric method for the determination of protein. *J. Lab. Clin. Med.* 1956. **48:** 311–314.

43 **Harrison, R. A. and Lachmann, P. J.,** Complement technology. In **Weir, D. M., Herzenberg, L. A., Blackwell, C. and Herzenberg, L. A. (Eds.)** *Handbook of Experimental Immunology.* Blackwell, London 1986.

44 **Oppermann, M., Schulze, M. and Gotze, O.,** A sensitive enzyme immunoassay for the quantitation of human C5a/C5a(desArg) anaphylatoxin using a monoclonal antibody with specificity for a neoepitope. *Complement Inflamm.* 1991. **8:** 13–24.

45 **Tedesco, F., Pausa, M., Nardon, E., Introna, M., Mantovani, A. and Dobrina, A.,** The cytolytically inactive terminal complement complex activates endothelial cells to express adhesion molecules and tissue factor procoagulant activity. *J. Exp. Med.* 1997. **185:** 1619–1627.

46 **Vita, F., Borelli, V., Soranzo M. R., Magnarin, M., Bertoncin, P. and Zabucchi, G.,** Preparation of membrane fractions from human neutrophil granules: a simple method. *Methods Cell Sci.* 1997. **19:** 197–205.

Correspondence: Francesco Tedesco, Dipartimento di Fisiologia e Patologia, Università di Trieste, Via Fleming 22, I-34127 Trieste, Italy
Fax: +39-040-567862
e-mail: tedesco@univ.trieste.it

ASBMB JOURNAL OF LIPID RESEARCH

Evolution of mammalian apolipoprotein A-I and conservation of antigenicity: correlation with primary and secondary structure

Xavier Collet,[1,*,†] Yves L. Marcel,[†] Nathalie Tremblay,[†] Claude Lazure,[§] Ross W. Milne,[†] Bertrand Perret,[*] and Philip K. Weech[†]

INSERM U326,* Hôpital Purpan, Toulouse Cedex 31059, France; Lipoprotein and Atherosclerosis Group,[†] Room H-460, University of Ottawa Heart Institute, Ottawa Civic Hospital, 1053 Carling Avenue, Ottawa, Ontario, Canada, K1Y 4E9; and Institut de Recherches Cliniques de Montreal,[§] 110 Avenue des Pins, Ouest, Montreal, Quebec, Canada H2W 1R7

Abstract We have evaluated the immunoreactivity of 20 monoclonal antibodies (mAbs) directed against human apolipoprotein (apo)A-I with a panel of high density lipoproteins (HDL) from 13 mammalian species. The pattern of cross-reactivity showed that 20 mAbs had different specificity. While not all mAbs recognized apoA-I from all of the different species, the antigenicity of some sequences was well conserved. Thus, mAb A05 cross-reacted with all species except guinea pig and rat. In contrast, the mAb 4H1, which recognized residues 2–8, required a specific proline in position 3, as no immunoreactivity was found in the species missing this amino acid. Furthermore, the presence of a threonine residue in place of serine (in position 6) in the cynomolgus monkey was associated with a 20-fold loss of immunoreactivity in radioimmunometric assay with 4H1. As most of the epitopes were found in CNBr fragments 2 and 3, we sequenced these regions in four species (horse, goat, sheep, and cat) and analyzed the alignment of most known sequences to evaluate their consensus. Except for the rat and the chicken, considerable identity was observed. This permitted us to deduce the involvement of the residues in some antigenic epitopes. In the middle of apoA-I, a conservative mutation $Asp_{109} \rightarrow Glu$ was found sufficient to eliminate all reactivity of this epitope for A11 (residues 99–105 . . . 126–132) in five species (rabbit, cow, goat, sheep, and rat). The residues essential to the expression of two other epitopes overlapping with A11 were also characterized. Edmundson-wheel representation of 18-residue repeated sequences of the different apoA-I species (for the eight amphipatic helices of residues 46–63, 68–85, 101–118, 123–140, 143–160, 167–184, 189–206, and 222–239) showed that secondary structure of apoA-I was more conserved than the antigenic epitopes. The N-terminal region, residues 1 to about 98, is rich in both strictly preserved sequences and epitope expression in most of the species surveyed. This evolutionary conservation of the N-terminal domain suggests an important yet unknown function.—**Collet, X., Y. L. Marcel, N. Tremblay, C. Lazure, R. W. Milne, B. Perret, and P. K. Weech.** Evolution of mammalian apolipoprotein A-I and conservation of antigenicity: correlation with primary and secondary structure. *J. Lipid Res.* 1997. 38: 634–644.

Supplementary key words apoA-I • monoclonal antibody

Apolipoprotein A-I (apoA-I), the principal protein constituent of high density lipoprotein (HDL) (1), is believed to be important in plasma cholesterol transport (2 and see review 3), and lecithin:cholesterol acyltransferase (LCAT) activation (4). Human apoA-I consists of a single 243 residue polypeptide (1) and its primary structure has also been determined in many species such as cynomolgus monkey, rat, rabbit, chicken, dog, pig, cow, and recently in the mouse (5–7 and see review 8). A high degree of homology was observed between the sequences from these different species (6–10). Panels of monoclonal antibodies (mAbs) have been raised against human apoA-I (11, 12), and we have recently described the mapping of the antigenic sites for 29 mAbs on human apoA-I (13). The mapping of the epitopes on the primary sequence of apoA-I is important because mAbs have proven to be useful probes of apoA-I conformation at the surface of HDL (14, 15). Given the variety of mAbs available, we wanted to elucidate which mAbs cross-react with different animal species. These antibodies are very useful reagents to study apoA-I structure and, in some cases, the species sequence differences may help to map the residues that contribute to antigenic sites. Therefore, we present here data on *1*) the cross-reactivity of 20 mAbs with apoA-I from 13 mammalian species, *2*) a list of conserved antigenic epitopes, *3*) new partial amino-acid sequences of apoA-I from some species studied and their alignment with the known apoA-I, *4*) the sequence con-

Abbreviations: apoA-I, apolipoprotein A-I; HDL, high density lipoprotein mAb, monoclonal antibody.

[1]To whom correspondence should be addressed.

sensus that emerged, and 5) a comparison of the α-helices in an Edmunson wheel representation.

MATERIALS AND METHODS

Isolation of lipoproteins

Blood from different species was obtained at the Ecole Nationale Vétérinaire (Toulouse, France) and collected on disodium EDTA (1 mg/ml). Plasma was separated by low speed centrifugation at 1000 *g* for 20 min at 4°C. Sodium azide (0.01%) and phenylmethylsulfonyl-fluoride (1 mM) were immediately added and the samples were stored at −80°C under nitrogen. The lipoproteins were prestained with Sudan Black and separated by discontinuous gradient ultracentrifugation (16, 17).

Monoclonal antibodies (mAbs) against apoA-I and competitive radioimmunoassays

All the mAbs used in the present study have been described (13) and were obtained from mice immunized with human apoA-I or HDL (11, 12). Solid phase radioimmunoassay of apoA-I without Tween 20 was carried out as described earlier (15).

Dot-blot

The interaction between monoclonal antibodies and the apoA-I from different species was studied by spotting onto nitrocellulose 2 μg of HDL protein in 2 μl. The nitrocellulose paper was saturated with 3% polyvinylpyrrolidone (44,000 mol wt; BDH Inc., Montreal, Quebec) in Tris-buffered saline (1 h, 37°C) and further processed as described previously (13). Autoradiography was performed on XAR-5 film (Eastman Kodak Co., Rochester, NY) with an intensifier screen (Cronex; DuPont Instruments, Wilmington, DE). Images were digitized and volume integration of immunoreactive dots was made using a Molecular Dynamics Computing Densitometer, with correction for the background adjacent to each blot.

Purification and CNBr treatment of apolipoprotein A-I

ApoHDL (20 μg) from different species were electrophoresed in a 15% acrylamide gel (18). The proteins were transferred onto nitrocellulose and apoA-I was identified by immunoreaction. To determine internal amino acid sequences, apoA-I was treated with cyanogen bromide (CNBr) as described previously (11). ApoA-I was eluted from the membranes with 500 μl of formic acid (98%), diluted with water to 70%, and 2.5 mg of CNBr (25 mg/ml) was added. The mixture was purged with nitrogen for 2 min and incubated overnight in the dark at room temperature. The polypeptide fragments were separated as described before and electrotransferred to PVDF membranes (Immobilon) (11).

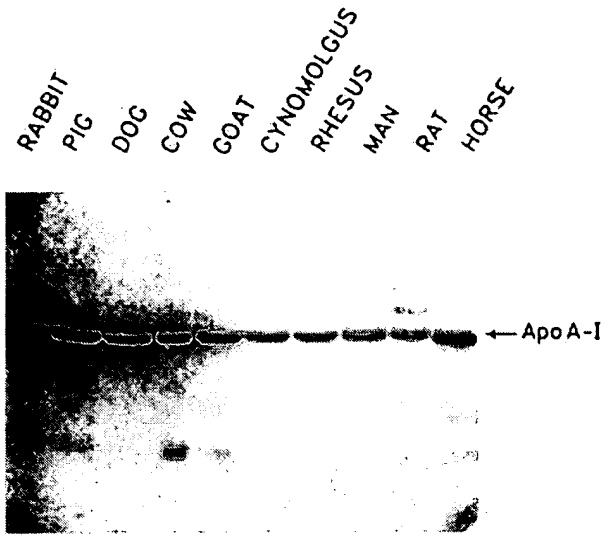

Fig. 1. SDS-PAGE of animal HDL protein (10 μg) electrotransfered onto nitrocellulose and stained with Ponceau red.

Analytical techniques

Complete protein sequences of human (APA1_HUMAN), cynomolgus monkey (APA1_MACFA), hamadryas baboon (APA1_PAPHA), rat (APA1_RAT), rabbit (APA1_RABIT), chicken (APA1_CHICK), dog (APA1_CANFA), bovine (APA1_BOVIN), pig (APA1_PIG), and mouse (APA1_MOUSE) apoA-I were from the SWISS protein sequence Data Bank (version 25). New amino acid sequences presented here were determined using an Applied Biosystems 470A sequencer with on-line PTH amino acid identification. Proteins were measured according to the method of Lowry et al. (19).

RESULTS

The lipoproteins from 13 animal species have been separated by discontinuous gradient centrifugation and the HDL were isolated. After SDS-PAGE separation, animal HDL proteins were electrotransferred onto nitrocellulose and stained with Ponceau Red. A major band of molecular weight of about 28,000 Da was visible in each sample (**Fig. 1**). Twenty three mAbs were tested for their reactivity with various apoA-I and HDL by dot-blot and Western blot. All the mAbs reacted with hu-

ASBMB JOURNAL OF LIPID RESEARCH JLR

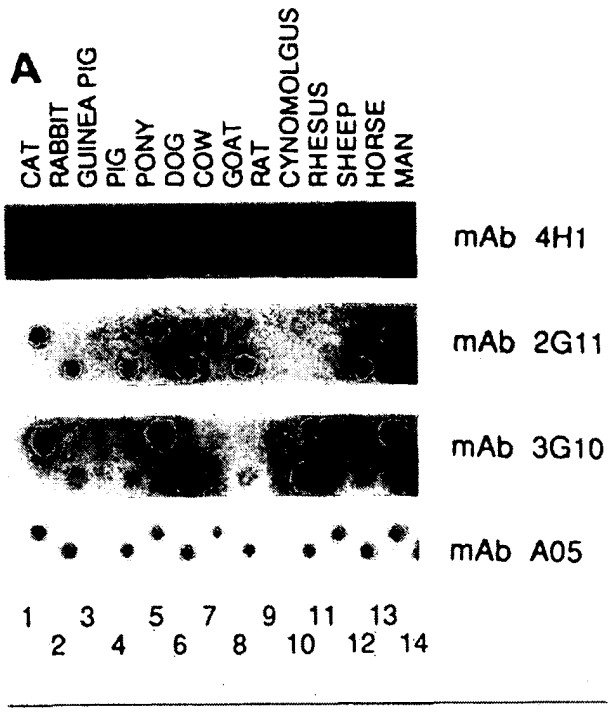

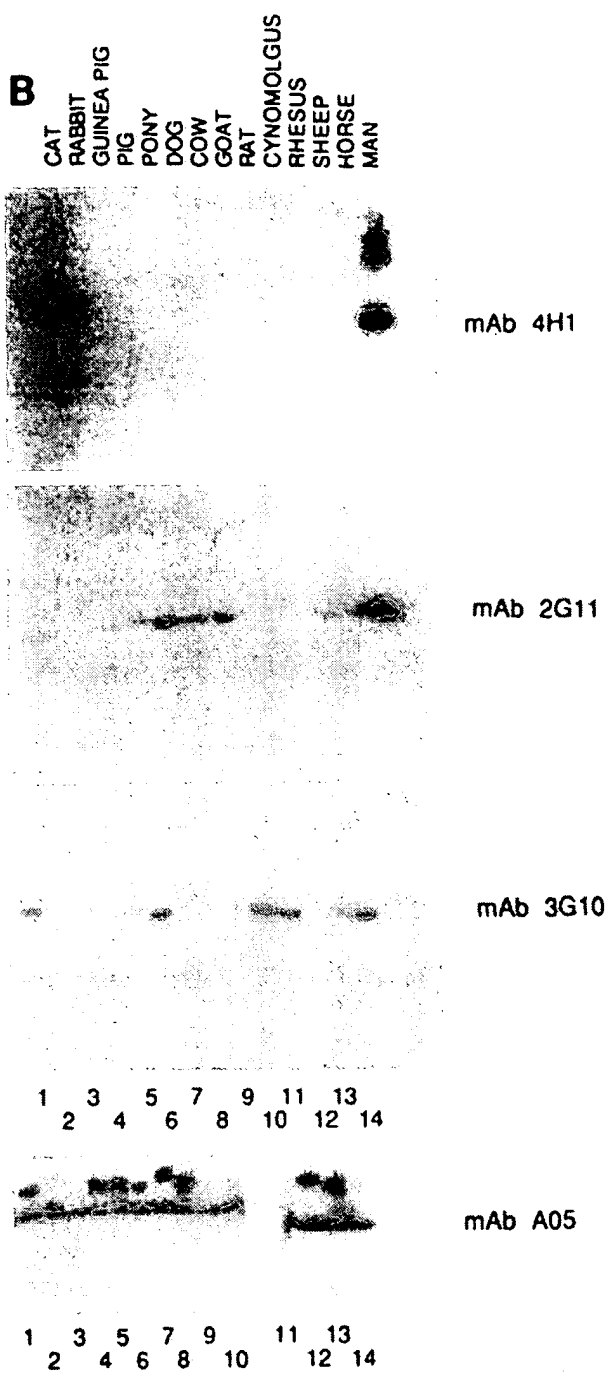

Fig. 2. A: Immunoreaction of four representative mAbs (4H1, 2G11, 3G10, and A05) with dot-blots of HDL (2 μg protein from various species) on nitrocellulose. B: Western blotting after SDS-PAGE of HDL (20 μg) with the same mAbs.

man apoA-I. The mAbs generally showed less reaction with HDL from the animal species than with human HDL in dot blots (**Fig. 2A**), and the same ranking order of reactivity was seen for animal apoA-I on Western blots after SDS-PAGE (Fig. 2B). While some species gave a strong reaction similar to human HDL, other species gave either weaker reactions or no detectable reaction over the background. The ranking order of reactivity of animal HDL was characteristically different for most of the mAbs. Out of the 20 different antibodies and the 13 different species, we found complete different patterns of reactivity (**Fig. 3** and **Table 1**). Thus a panel of different mammalian HDL allows rapid screening to identify differences among antibodies with unique specificities. Antibodies 4H1, 6B8, A10, and 4A12 reacted only with human, rhesus, and cynomolgus apoA-I. The mAb 4H1 recognizes a single linear epitope in the amino terminal region of human apoA-I spanning residues 2–8 (13) (Fig. 3 and Table 1). The antibody 4H1 requires a specific amino acid (Pro) in position 3 or 4, that is absent in the majority of species other than human (through deletion or mutation). Serine in position 6 appears important, as a substitution ($Ser_6 \rightarrow Thr$) led to a low immunoreactivity with apoA-I from the cynomolgus and rhesus monkeys. This was verified by competition radioimmunoassay, in which apoA-I from cynomolgus and rhesus HDL was about 20-fold less immunoreactive with 4H1 than with that of human

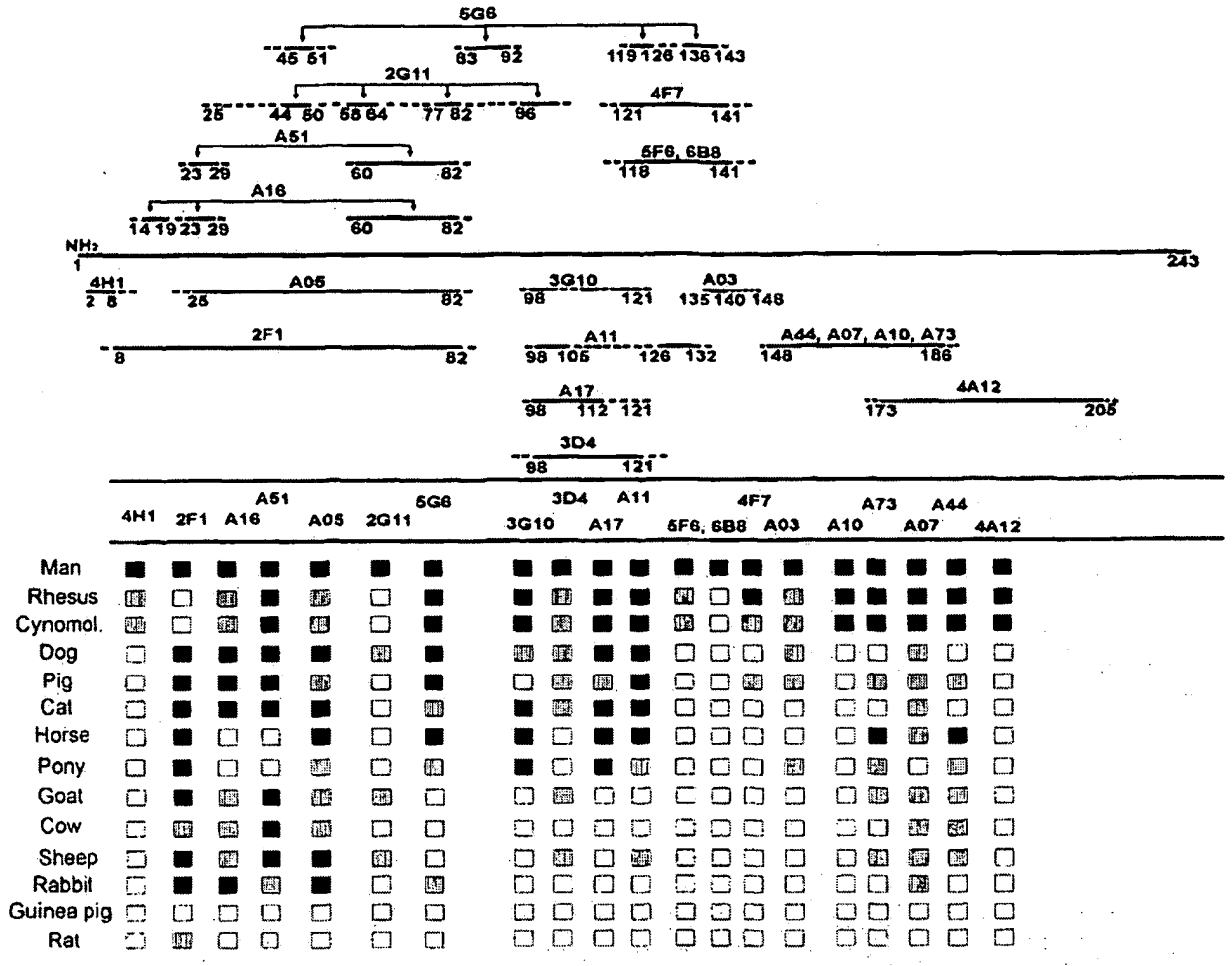

Fig. 3. Epitope map of apolipoprotein A-I and comparison of the immunoreactivity of 20 monoclonal antibodies with the apoA-I of different animal species. The data are consistent with both dot-blots of HDL and SDS-PAGE Western blots of HDL. Filled squares, immunoreaction with intensity comparable to the human sample (range 50–100% in Table 1); hatched squares, immunoreactivity with intensity less than the human sample (range 10–49% in Table 1); and open squares, no significant immunoreaction (0–9% in Table 1).

TABLE 1. Immunoreactivity of apoA-I in different species relative to that in humans

	4H1	2F1	A16	A51	AO5	2G11	5G6	3G10	3D4	A17	A11	5F6	6B8	4F7	AO3	A10	A73	A07	A44	4A12
Human	100	100	100	100	100	100	100	100	100	100	100	100	100	100	100	100	100	100	100	100
Rhesus	43	0	44	89	45	0	52	76	44	64	69	24	0	61	26	63	85	90	95	87
Cynomol.	35	0	47	92	41	0	58	61	40	77	74	26	0	46	36	78	72	78	81	70
Dog	0	105	59	60	60	14	63	49	24	99	71	10	0	2	22	3	2	27	0	0
Pig	0	87	52	88	44	8	50	0	38	11	53	4	0	11	15	1	26	23	21	0
Cat	0	78	77	94	68	6	34	75	30	81	78	0	0	1	4	0	4	36	0	0
Horse	0	72	0	0	50	8	71	68	9	68	71	1	0	5	0	0	50	14	61	0
Pony	0	81	0	0	45	9	42	68	6	63	43	0	0	4	12	0	47	8	45	0
Goat	0	93	36	58	38	14	1	0	12	7	7	0	0	5	5	2	22	29	29	0
Cow	0	43	21	55	29	9	0	0	5	6	5	0	0	4	7	2	0	21	16	0
Sheep	0	72	23	148	51	15	0	0	14	0	16	0	0	4	0	0	23	36	30	0
Rabbit	0	99	54	37	55	10	42	0	5	3	2	0	0	9	8	0	5	22	0	0
Guinea pig	0	0	0	0	1	0	0	0	0	7	4	0	0	0	3	0	3	0	0	0
Rat	0	49	0	0	1	0	0	4	9	5	8	0	0	1	0	1	0	0	0	0

Comparison of the immunoreactivity of 20 monoclonal antibodies with the apoA-I of different animal species. The data are consistent with both dot blots of HDL and SDS-PAGE Western blots of HDL. Images were digitized and surface integration of the immunoreactive dots was made using a Molecular Dynamics Computing Densitometer, with correction for the background adjacent to each blot.

JOURNAL OF LIPID RESEARCH ASBMB

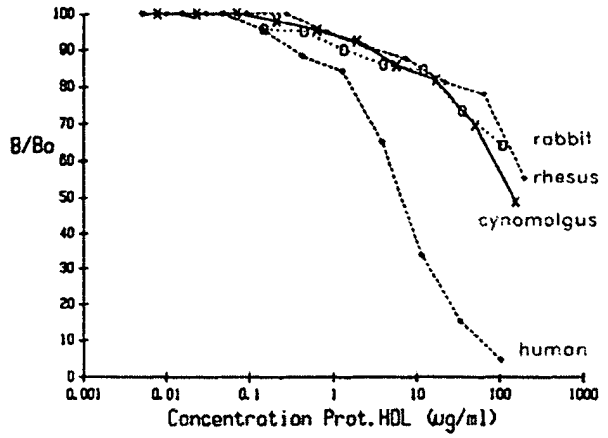

Fig. 4. Comparison of the immunoreactivity of human, cynomolgus, rhesus monkey, and rabbit HDL with monoclonal antibody 4H1 by competitive radioimmunoassay.

(Fig. 4). In the middle of the apoA-I sequence, a substitution $Asp_{103} \rightarrow Glu$ was found sufficient to eliminate any reactivity of this epitope for mAb A11 (residues 99–105 . . . 126–132) in six species (rabbit, cow, goat, sheep, rat, and guinea pig), whereas all species with Asp_{103} have highly reactive HDL. Antibody A17 which reacts with an epitope overlapping with A11 but which is more defined to the sequence 98–112, displays the same specificity, further supporting the role of Asp_{102}. Asp_{103} appears important also for antibody 3G10 which recognizes fragments 98–103 and 110–119 and is immunoreactive with the different species recognized by mAb A11 with the exception of the pig (Fig. 3). In addition to Asp_{103}, two other amino acids, Ala_{95} and Lys_{106}, could be involved in the immunoreactivity of mAb A11. Immunoreactive species with 3G10 express alanine or glutamine at position 95 and pig does not. However, pig also expresses Asn_{106} instead of lysine (Fig. 5).

In order to obtain some sequences of apoA-I fragments from goat, sheep, cat, and horse, which are not yet available, apoA-I were treated by CNBr. Different fragments were separated by electrophoresis. As previously described, apoA-I CNBr fragmentation was incomplete (not shown). Two gels were run in parallel, one was used for silver staining and the other was blotted with mAb A05. This antibody was shown to react with all species except for the rat and the guinea pig (see Table 1), and it is specific for human apoA-I CNBr fragment 2 (12). Amino acid sequences were determined after electrotransfer of the apoA-I CNBr fragments onto membranes. The apoA-I sequences from some species are presented in Fig. 5. We obtained for the goat and sheep, sequences at the NH_2 terminus (residues 1–13 and 1–21, respectively) and also for the goat, sheep, and cat, sequences starting from position 86 (86–115, 86–116, and 86–111, respectively), and corresponding to CNBr fragment 2. Concerning horse apoA-I, one fragment was sequenced between residues 148 and 178, in CNBr fragment 2.

ApoA-I contains about the same number of basic residues, 28, and of acidic ones, 20. The NH_2 terminus of apoA-I contains many more basic residues (10 out of the first 51 amino acids) than acidic ones (3 residues). The protein contains 54 conserved hydrophobic residues (22%). Although the hydrophobic amino acids are distributed over the entire protein, there is, however, a greater concentration at the NH_2 terminus (18 of the first 60 residues). It is noteworthy that there are 3 conservative and consecutive hydrophobic amino acids VYV at positions 17–19. The two sequences most conserved in all species (18 and 13 amino acids) and where only homologous substitutions occur, are between residues 22–39 and 47–59. The sequences for which a strict conservation has been noted in eight different species are mostly found in the N-terminal half and include residues 17–19 (as noted above), residues 23–26, residues 32–34, residues (NLEKET) at positions 74–79, and residues 88–90. There are also a number of short amino acid sequences that are well conserved (64–68, 86–90, 96–99, 101–105, 115–119, 191–196, 203–209, and 216–224). This preponderance of well-conserved sequences in the N-terminal region is compatible with the well-conserved immunoreactivity of N-terminal epitopes in the different species. Indeed, out of seven epitopes characterized toward the N-terminus, only 4H1 and 2G11 react with only 3 and 4 species, respectively, while the others react with 9 or more species. Particularly noteworthy are antibodies 2F1 and A05 whose epitopes overlap between residues 8–82 and 25–82, and which react with 11 and 12 species out of the 14 tested. As indicated above, it is within this sequence that are found strictly conserved sequences (residues 17–19, 23–26, 32–34, and 74–79) and the sequence 46–51 which is also strictly conserved in all species but the mouse, where a conservative substitution, Asp48 to Glu, occurs.

We attempted to compare the conservation of different helical segments of apoA-I among various species as designed by Brasseur (20) using the Edmunson-wheel diagram (Fig. 6). The loop formed between helices 1 and 2 has the sequence-XGPXT- where X represents a hydrophobic amino acid (residue 64–68) and contains no charged amino acids (Fig. 5). Another sequence-UULXPXL- (where U represents an uncharged amino acid, H, Q, S, or G) in the loop between helices 7 and 8 (residues 216–222) displays no ionized residue. A very interesting conservation is observed in the helix 167–184 where there is a very well-conserved global charge upon two turns of the wheel (Fig. 6). In

position 172 there is a glutamic acid (red color) in dog, rat, and mice, and a glutamine in human, cynomolgus monkey, rabbit, cow, chicken, and pig, whereas in position 179 there is a glutamic acid in human, cynomolgus, rabbit, cow, chicken, and pig and a glutamine (dog), a threonine (rat) and an alanine (mice) (uncolored). However, the comparison of sequences using the Edmunson-wheel diagram did not help to further identify the epitopes and their conservation, possibly owing to the earlier report that most epitopes in this region of apoA-I appeared centered around the turns (13).

DISCUSSION

Epitopes may depend on protein conformation as well as amino acid sequence and for that reason, comparison of primary structure does not always allow us to uniquely assign each epitope. Furthermore, most characterized protein epitopes are composed of discontinuous regions of polypeptides (21–23), and this has been observed for many apoA-I epitopes, especially in the N-terminal half (13). Although the antibodies analyzed here did not include mAbs specifically selected to react with linear epitopes as described recently by Curtiss and Banka (24), we have identified, by comparison of sequences and epitope expression in different species, specific residues that are critical to the expression of several epitopes.

In the present study, we have compared apoA-I from different animal species that differ from human apoA-I only by a few amino acids. These differences have been used to map the residues that contribute to the immunogenicity of apoA-I. Pro_5 has been shown to be essential for the expression of the 4H1 epitope. It is noteworthy that this region of the sequence is hypervariable, as natural mutants have been described with proline deletion at position 3 or 4 of human apoA-I (9). This antibody may be useful to detect these natural mutations in human apoA-I. Several mouse mAbs react with overlapping epitopes spanning the residues 80–140 (Fig. 3). This region represents the main immunogenic region of apoA-I as suggested by Curtiss and Banka (24) using the Chou and Fasman algorithms (25) for prediction of antigenicity. We had also shown earlier that several epitopes are centered around the α-helix predicted between residues 99–121 (13), a region that we proposed to be a hinge domain (26). Three epitopes overlapping this sequence have been further delineated: Asp_{103} is essential to the expression of the epitopes for both A11 and A17, whereas the epitope for 3G10 requires not only Asp_{103} but also Ala_{95} and/or Asn_{106}. The antigenicity of this domain can be explained by its mobility and accessibility to proteolysis (27). Downstream of this sequence, Ehnholm and colleagues (28) identified a mAb that reacts with normal apoA-I but not with a genetic variant of apoA-I ($Glu_{136} \rightarrow Lys$). This point mutation induced a lack of immunoreactivity of the mAb with the epitope located between residues 113 and 148. Indeed residue 136 is close to a proline at position 139 which is thought to interrupt the amphipathic helix. This is in keeping with our earlier report (13) that many of the helix breaking regions of apoA-I constitute antigenic domains. Downstream of the putative hinge domain between residues 121 and 180, there is little in the way of consensus sequences or even consensus residues although most of the substitutions are conservative (Fig. 5). There is also little conservation of epitopes between species and no other epitope could be further delineated (Fig. 3).

We have observed that, in contrast in the N-terminal half of apoA-I, a number of epitopes are expressed consistently in most of the species studied (Fig. 3) and thus appear conserved through evolution. The strict conservation of a number of sequences distributed in this region probably explains the epitope conservation in the N-terminal region. With the exception of antibody 4H1, most epitopes at the extreme N-terminus have been shown to be discontinous (13). The presence of the discontinuous epitopes is also compatible with the observations and model of Nolte and Atkinson (29) who noted that the N-terminus domain (residues 1–57) contains the most ambiguously defined secondary structures. The model of the N-terminal region presented by these authors very interestingly suggests a complex tertiary structure based on amphipathic β-sheet where some of the strictly conserved sequences (residues 17–19 and 42–44) are found that are separated by random coil sequences also strictly conserved (residues 23–26 and 46–51).

The natural selection that favors the conservation of functionally important proteins is a widely accepted idea in evolutionary theory. The antigenicity index of an important and invariant functional domain in protein is very low whereas the regions outside the functional domain vary and can be highly antigenic. As well, primary structures, and thus antigenic epitopes, that may have important metabolic functions are conserved in a variety of species. In keeping with this principle, Nelson et al. (30) noted that epitopes spatially located near the recognition site of apoB have a greater tendency to be conserved in a variety of animal species, a result confirmed by Young et al. (31). The carboxyterminal region with its two α-helices at residues 189–206 and 222–239 is a highly conserved part of the apoA-I molecule (Figs. 5 and 6), and only two antibodies have been reported to bind to this region (32). This low anti-

JOURNAL OF LIPID RESEARCH ASBMB

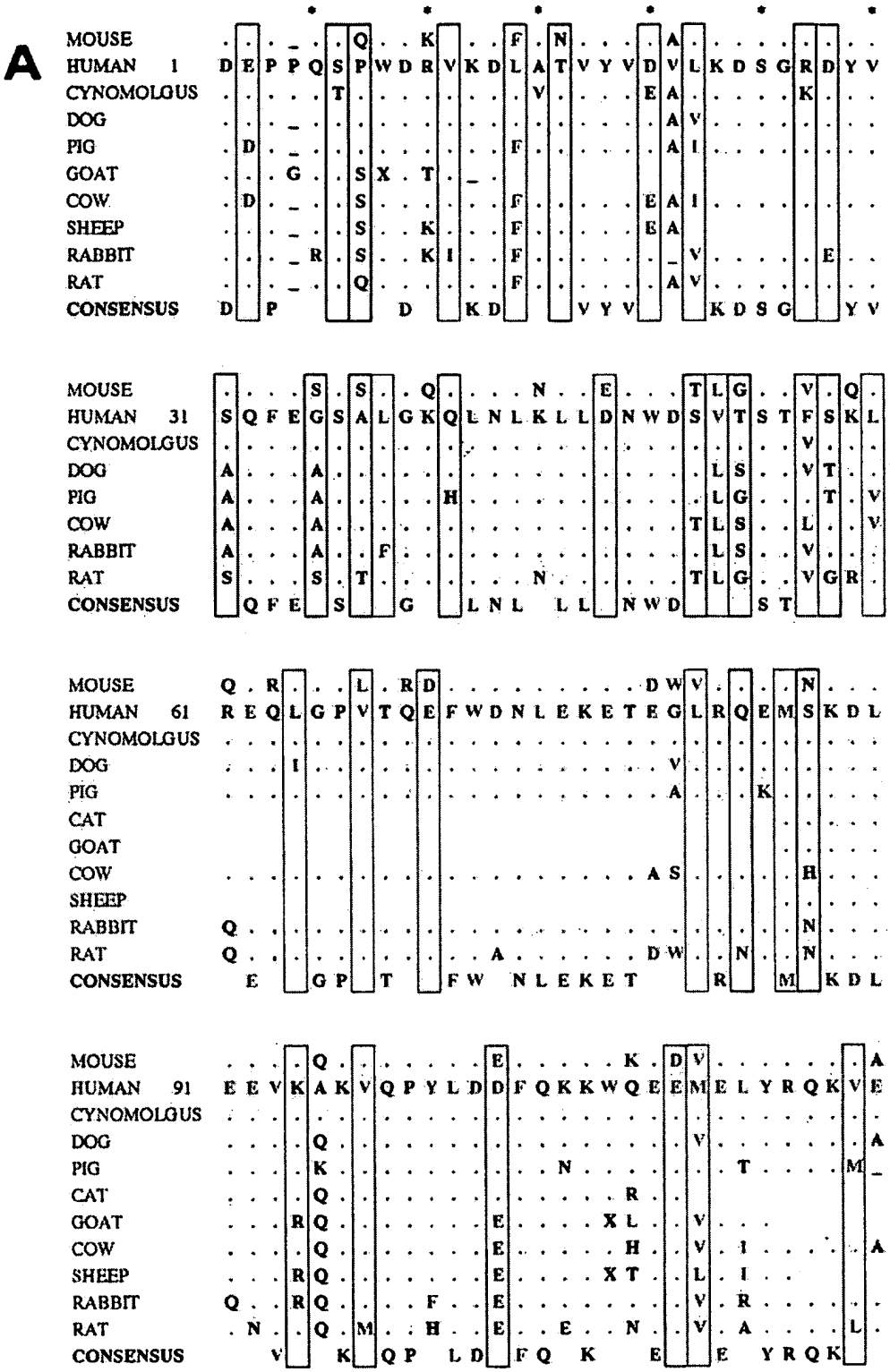

Fig. 5.

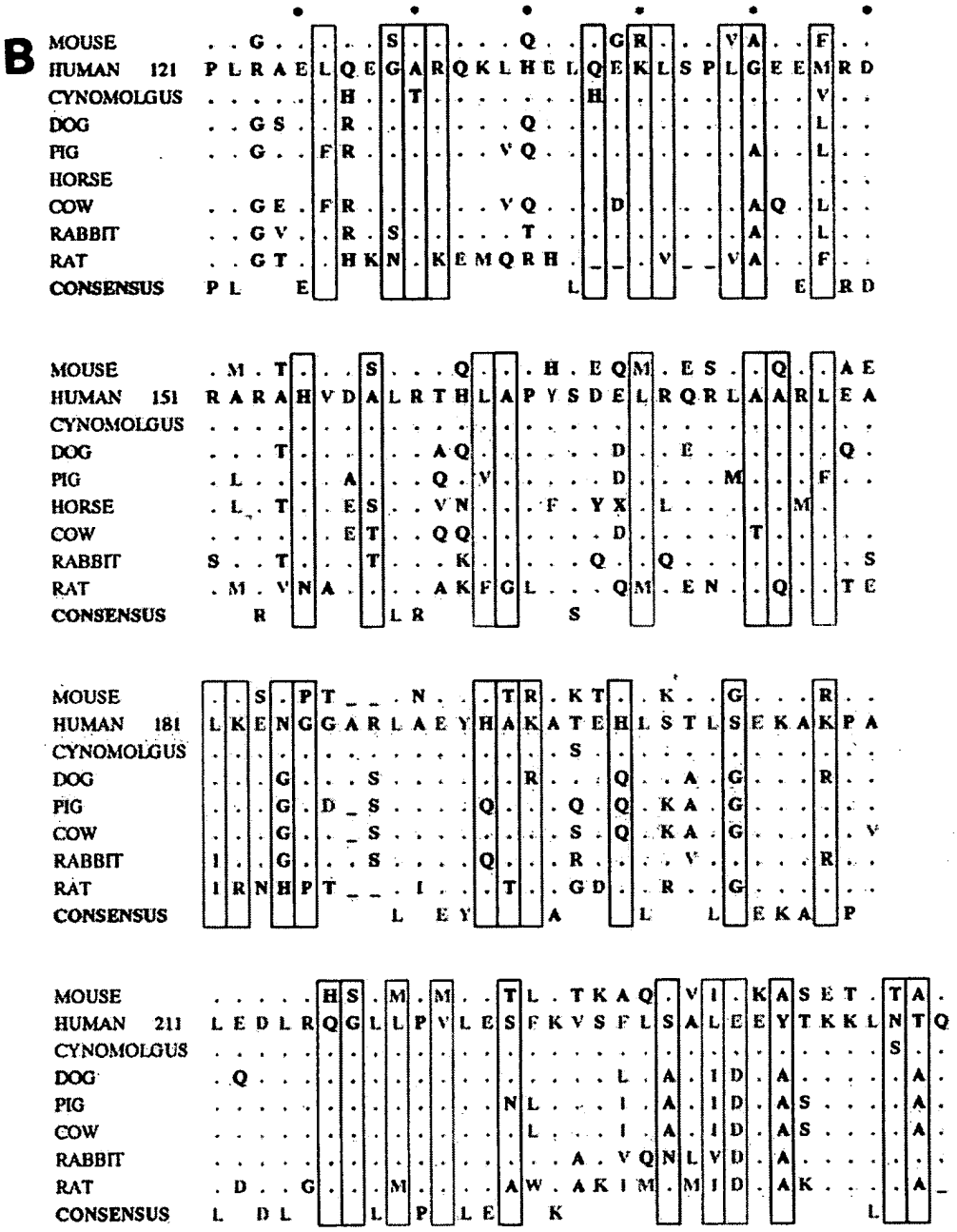

Fig. 5. Comparison of apoA-I amino acid sequences. Colors indicate aspartic acid or glutamic acid (red, D and E); arginine or lysine (blue, R and K); and hydrophobic residues methionine, valine, leucine, isoleucine, phenylalanine, tyrosine, or tryptophan (green, M, V, L, I, F, Y, and W). The remaining neutral amino acids at physiological pH, glycine, alanine, serine, threonine, asparagine, glutamine, histidine, and cysteine (G, A, S, T, N, Q, H and C) are uncolored. The column containing amino acids of the same color that possess the same character are boxed.

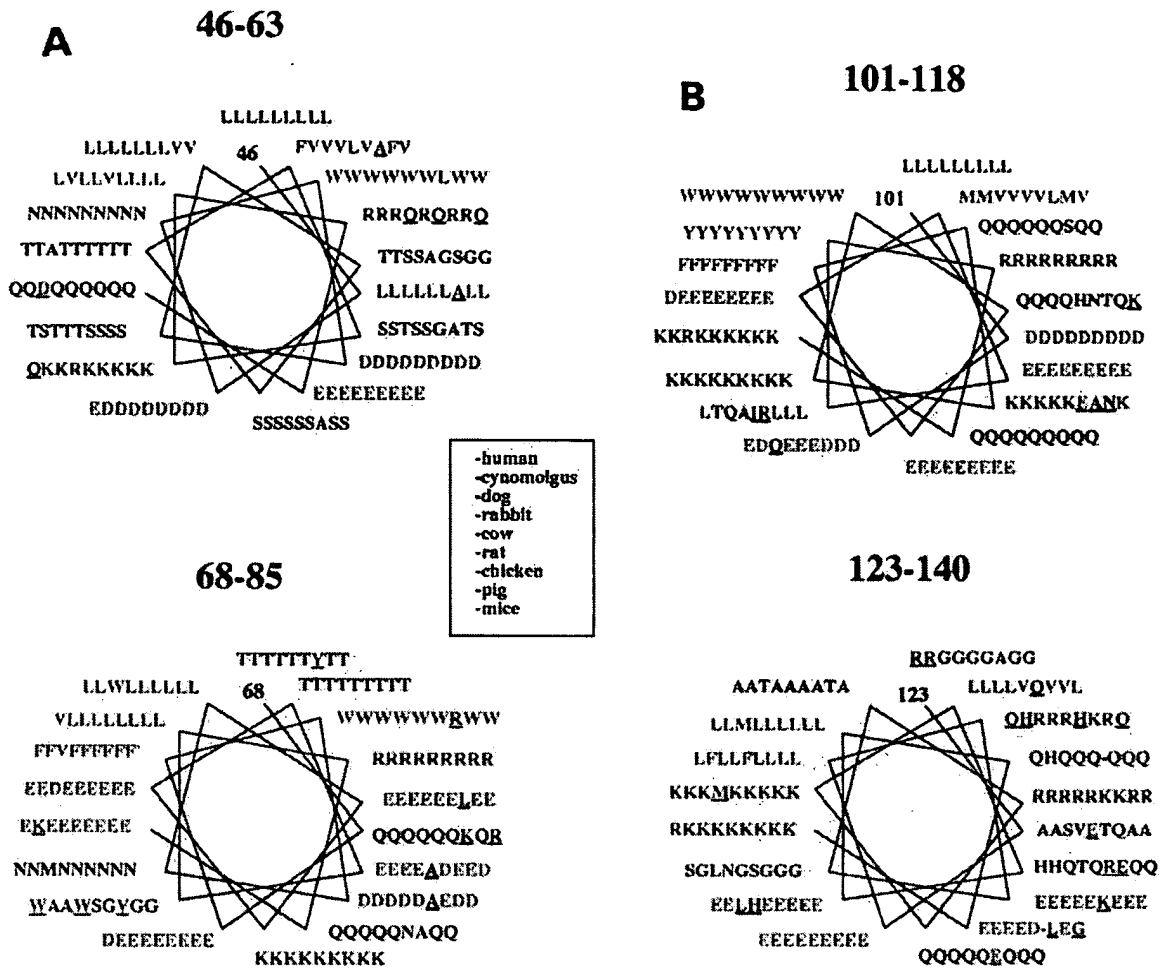

Fig. 6. Edmundson-wheel diagram of 18-residue repeated sequences of the different apoA-I species from human, cynomolgus, dog, rabbit, cow, rat, chicken, pig, and mice. Amino acids at each position are listed from inside to the exterior of the wheel, in the order in which these proteins are listed. Eight amphipathic α-helices are represented 46–63, 68–85, 101–118, 123–140, 143–160, 167–184, 189–206, and 222–239. The colors correspond to these of Fig. 5. The amino acids that possess a different character are underlined.

genicity may be related to the evolutionary preservation of this segment. Alternatively, the carboxyl-terminal domain that is the main lipid binding domain (33) may also have undergone many silent mutations which, while preserving its functionality, i.e., the amphipathic characteristics of α- helices, did not preserve the immunoreactivity. In contrast, it is clear from the summary of cross-species expression of epitopes in Figs. 3 and 5, that there is a highly preserved set of overlapping epitopes in the N-terminal domain, essentially between residues 25 and 82. This may reflect the conservation of a domain with a complex tertiary structure which must serve an important but yet unknown function.

Analysis of evolutionary relationships among different apoA-I sequences shows that apoA-I is a highly conserved protein (7–9). The major ambiguity in any sequence alignment concerns the insertions that are required to improve the overall alignment. The insertions and/or deletions generally occur in the more variable loop regions of the structure. Estimates of substitution rates show that apoA-I evolved about 25% faster than an average gene in mammalian lineage as already calculated by Januzzi et al. (6). However, all portions of the coding regions evolve at roughly similar rates, suggesting that global conformation is conserved. This is corroborated by a conservation of the substituted amino acids of similar character (Fig. 5).

In conclusion, we have identified in this report the

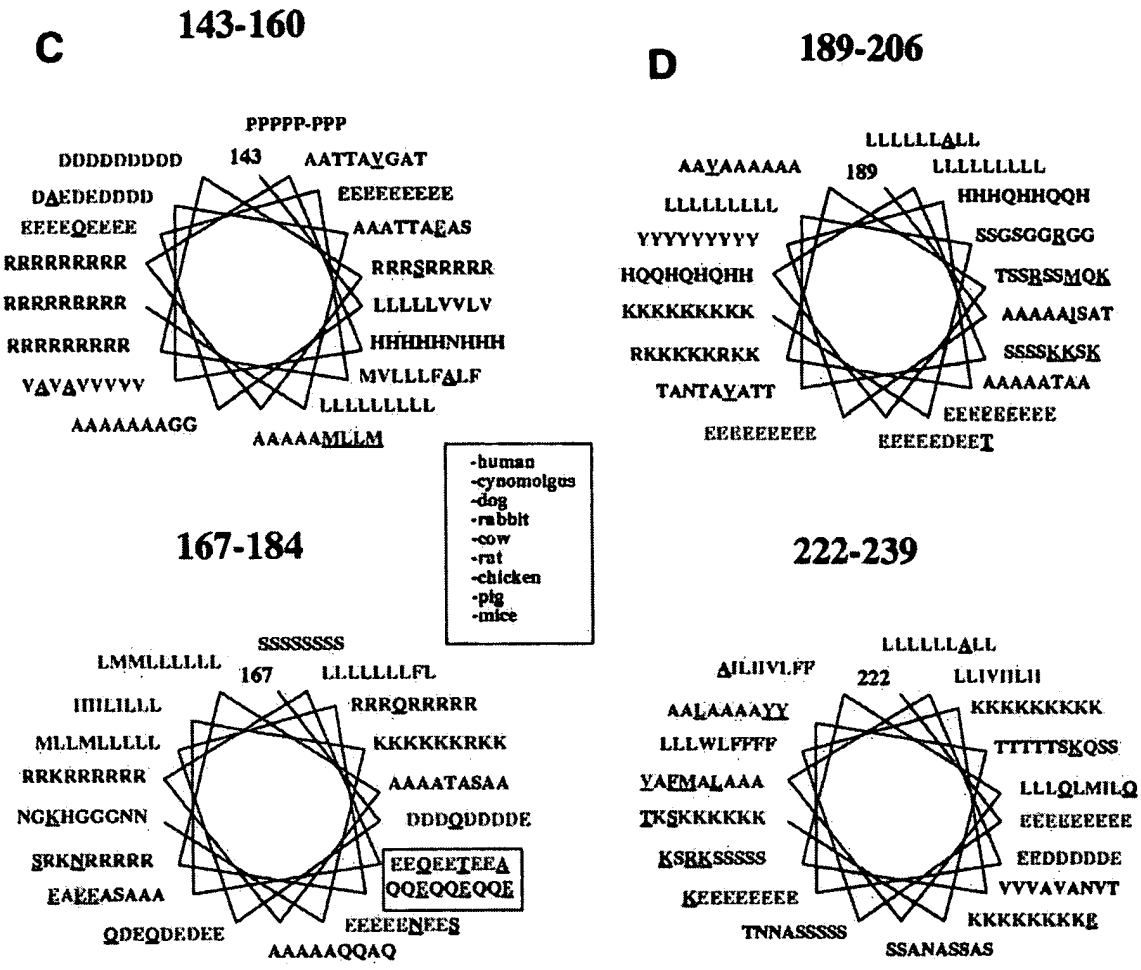

Fig. 6.

mAbs that cross-react with apoA-I of different animal species and defined further some of their epitopes. This enables us to select the mAbs that are appropriate for studies of apoA-I in animal species, to define more precisely some antigenic sites, and, finally, to identify conserved structures in apoA-I. This approach may help us to understand the evolution of apoA-I and other exchangeable apolipoproteins.

We acknowledge Pr. J.C. Fruchart for providing some of the mAbs against human apoA-I and Dr. Patrick Benard at the Ecole Nationale Vétérinaire (Toulouse) for providing the plasma samples of animal species. We thank Pr. Hugues Chap and Dr. Ronald Barbaras for valuable discussion and a critical reading of this manuscript. This study was supported in part by a group grant from the Medical Research Council of Canada.

Manuscript received 23 May 1996 and in revised form 25 November 1996.

REFERENCES

1. Brewer, H. B., Jr., T. Fairwell, A. La Rue, B. Ronan, A. Houser, and T. J. Bronzert. 1978. The amino acid sequence of human ApoA-I, an apolipoprotein isolated from high density lipoproteins. *Biochem. Biophys. Res. Commun.* **80:** 623–630.
2. Miller, N. E., A. Laville, and D. Crook. 1985. Direct evidence that reverse cholesterol transport is mediated by high density lipoprotein in rabbit. *Nature.* **314:** 109–111.
3. Fielding, C. J., and P. E. Fielding. 1995. Molecular physiol-

ogy of reverse cholesterol transport. *J. Lipid Res.* **36:** 211–228.
4. Fielding, C. J., V. G. Shore, and P. E. Fielding. 1972. A protein cofactor of lecithin:cholesterol acyltransferase. *Biochem. Biophys. Res. Commun.* **46:** 1493–1498.
5. Weiler-Guttler, H., M. Sommerfeldt, A. Papandrikopoulos, U. Mischek, D. Bonitz, A. Frey, M. Grupe, J. Scheerer, and H. G. Gassen. 1990. Synthesis of apolipoprotein A-I in pig brain microvascular endothelial cells. *J. Neurochem.* **54:** 444–450.
6. Januzzi, J. L., N. Azrolan, A. O'Connell, K. Aalto-Setälä, and J. L. Breslow. 1992. Characterization of the mouse apolipoprotein Apoa-1/apoc-3 gene locus: genomic, mRNA, and protein sequences with comparisons to other species. *Genomics.* **14:** 1081–1088.
7. O'hUigin, C., L. Chan, and W-H. Li. 1990. Cloning and sequencing of bovine apolipoprotein A-I cDNA and molecular evolution of apolipoproteins A-I and B-100. *Mol. Biol. Evol.* **4:** 327–339.
8. Luo, C. C., W. H. Li, and L. Chan. 1989. Structure and expression of dog apolipoprotein A-I, E, and C-I mRNAs: implications for the evolution and functional constraints of apolipoprotein structure. *J. Lipid Res.* **30:** 1735–1746.
9. von Eckardstein, A., H. Funke, M. Walter, K. Atland, A. Benninghoven, and G. Assmann. 1990. Structural analysis of human apolipoprotein A-I variants. Amino acid substitutions are nonrandomly distributed throughout the apolipoprotein A-I primary structure. *J. Biol. Chem.* **265:** 8610–8617.
10. Brasseur, R., J. De Meutter, B. Vanloo, E. Goormaghtigh, J. M. Ruysschaert, and M. Rosseneu. 1990. Model of assembly of amphipathic helical segments in model high-density lipoproteins. *Biochim. Biophys. Acta.* **1043:** 245–252.
11. Weech, P. K., R. W. Milne, P. Milthorp, and Y. L. Marcel. 1985. Apolipoprotein A-I from normal human plasma: definition of 3 distinct antigenic determinants. *Biochim. Biophys. Acta.* **835:** 390–401.
12. Petit, E., M. Ayrault-Jarrier, D. Pastier, H. Robin, J. Polonovski, I. Aragon, E. Hervaud, and B. Pau. 1987. Monoclonal antibodies to human apolipoprotein A-I: characterization and application as structural probes for apolipoprotein A-I and high density lipoprotein. *Biochim. Biophys. Acta.* **919:** 287–296.
13. Marcel, Y. L., P. R. Provost, H. Koa, E. Raffai, N. Vu Dac, J. C. Fruchart, and E. Rassart. 1991. The epitopes of apolipoprotein A-I define distinct structural domains including a mobile middle region. *J. Biol. Chem.* **266:** 3644–3653.
14. Curtiss, L. K., and R. S. Smith. 1986. Localization of two epitopes of apolipoprotein A-I that are exposed on human high density lipoproteins using monoclonal antibodies and synthetic peptides. *J. Biol. Chem.* **263:** 13779–13785.
15. Collet, X., B. Perret, G. Simard, E. Raffai, and Y. L. Marcel. 1991. Differential effects of lecithin and cholesterol on the immunoreactivity and conformation of apolipoprotein A-I in high density lipoproteins. *J. Biol. Chem.* **266:** 9145–9152.
16. Terpstra, A. H. M., C. J. H., Woodward, and F. Sanchez-Muniz. 1981. Improved techniques for the separation of lipoproteins by density gradient ultracentrifugation: visualization by prestaining and rapid separation of serum lipoproteins from small volumes of serum. *Anal. Biochem.* **111:** 149–157.
17. Weech, P. K., D. Jewer, and Y. L. Marcel. 1988. Apolipoprotein A-I assayed in human serum by isotope dilution as a potential standard for immunoassay. *J. Lipid Res.* **29:** 85–93.
18. Neville, D. M., Jr. 1971. Molecular weight determination of protein dodecyl sulfate complexes by gel electrophoresis in a discontinuous buffer system. *J. Biol. Chem.* **246:** 6328–6334.
19. Lowry, O. H., N. J. Rosebrough, A. L. Farr, and R. J. Randall. 1951. Protein measurement with the Folin phenol reagent. *J. Biol. Chem.* **193:** 265–275.
20. Brasseur, R. 1991. Differentiation of lipid-associating helices by use of three-dimensional molecular hydrophobicity potential calculations. *J. Biol. Chem.* **266:** 16120–16127.
21. Davies, D. R., S. Sheriff, and E. A. Padlan. 1988. Antibody-antigen complexes. *J. Biol. Chem.* **263:** 10541–10544.
22. Geysen, H. M., S. J. Rodda, and T. J. Mason. 1986. The delineation of peptides able to mimic assembled epitopes. *Ciba Found. Symp.* **119:** 130–49.
23. Barlow, D. J., M. S. Edwards, and J. M. Thornton. 1986. Continuous and discontinuous protein antigenic determinants. *Nature.* **322:** 747–748.
24. Curtiss, L. K., and C. L. Banka. 1996. Selection of monoclonal antibodies for linear epitopes of an apolipoprotein yields antibodies with comparable affinity for lipid-free and lipid-associated apolipoprotein. *J. Lipid Res.* **37:** 884–892.
25. Chou, P. Y., and G. D. Fasman. 1974. Prediction of protein conformation. *Biochemistry.* **13:** 222–245.
26. Calabresi, L., Q. H. Meng, G. R. Castro, and Y. L. Marcel. 1993. Apolipoprotein A-I conformation in discoidal particles: evidence for alternate structures. *Biochemistry.* **32:** 6477–6484.
27. Dalton, M. B., and J. B. Swaney. 1993. Structural and functional domains of apolipoprotein A-I within high density lipoproteins. *J. Biol. Chem.* **268:** 19274–19283.
28. Ehnholm, C., M. Lukka, I. Rostedt, and K. Harper. 1986. Monoclonal antibodies for different regions of human apolipoprotein A-I. Characterization of an antibody that does not bind to a genetic variant of apoA-I (Glu136 → Lys). *J. Lipid Res.* **27:** 1259–1264.
29. Nolte, R. T., and D. Atkinson. 1992. Conformational analysis of apolipoprotein A-I and E-3, based on primary sequence and circular dichroism. *Biophys. J.* **63:** 1221–1239.
30. Nelson, C. A., M. A. Tasch, M. Tikkanen, R. Dargar, and G. Schonfeld. 1984. Evolution of low density lipoprotein structure probed with monoclonal antibodies. *J. Lipid Res.* **25:** 821–830.
31. Young, S. G., J. L. Witztum, D. C. Casal, L. K. Curtiss, and S. Bernstein. 1985. Conservation of the low density lipoprotein receptor-binding domain of apolipoprotein B. Demonstration by a new monoclonal antibody, MB47. *Arteriosclerosis.* **6:** 178–188.
32. Fidge, N., J. Morrison, T. Nugent, and M. Tokusa. 1989. Monoclonal antibodies to human A-I apolipoprotein and characterisation of cyanogen bromide fragments of apoA-I. *Biochim. Biophys. Acta.* **1003:** 84–90.
33. Minich, A., X. Collet, A. Roghani, C. Cladaras, R. L. Hamilton, C. J. Fielding, and V. I. Zannis. 1992. Site-directed mutagenesis and structure-function analysis of the human apolipoprotein A-I. Relation between lecithin:cholesterol acyltransferase activation and lipid binding. *J. Biol. Chem.* **267:** 16553–16560.

EXHIBIT D

Proc. Natl. Acad. Sci. USA
Vol. 82, pp. 1508–1512, March 1985
Immunology

Analysis of an evolutionarily conserved antigenic site on mammalian cytochrome *c* using synthetic peptides

(*N*-acetylation/antigenic design/immunodominant)

RONALD JEMMERSON, PHILLIP R. MORROW, NORMAN R. KLINMAN, AND YVONNE PATERSON*

Department of Immunology, Scripps Clinic and Research Foundation, 10666 North Torrey Pines Road, La Jolla, CA 92037

Communicated by E. Margoliash, November 16, 1984

ABSTRACT **Two synthetic peptides inclusive of the NH_2-terminal *N*-acetyl-Gly-Asp-Val-Glu tetrapeptide of mammalian cytochrome *c* (cyt *c*) were used in this study to address the question of whether mammals can respond immunologically to an evolutionarily conserved region of a protein. These peptides were assessed for their capacity (*i*) to act as immunogens for the production of anti-self cyt *c* antisera and (*ii*) to bind rabbit anti-rodent cyt *c* antibody. The findings from these studies indicate the existence of an immunogenic determinant in an evolutionarily conserved region of cyt *c* that contains residues 1–4. This determinant can induce anti-self cyt *c* antibodies whether presented as a peptide on a carrier protein or in the context of the intact molecule as polymerized mammalian cyt *c*.**

A commonly accepted view of the antigenicity of a protein is that the predominant epitopes correspond to those regions where the immunizing protein differs in amino acid sequence from the homologous protein of the immunized animal (1). This concept followed directly from the phenomenon of immunological tolerance. If B cells having specificities for structures on self proteins are aborted or rendered tolerant, then only those B cells having specificities for foreign antigenic determinants should remain in a state that can be activated (2). This is obviously an oversimplification in that T cells and macrophage processing probably have a large effect on which parts of a protein will be antigenic in a particular host. Nonetheless, data obtained from recent studies, most notably with cytochrome *c* (cyt *c*), continue to support the hypothesis (3–6). Thus, for example, three different groups (4–6) found that the antigenic determinants on horse cyt *c*, as recognized by rabbits, correspond to three regions of the molecule—namely, around resides 44, 60, and 89/92, where horse and rabbit cyt *c* differ in amino acid sequence.

In apparent conflict with the hypothesis was the observation that antibodies could be elicited in rabbits against their own cyt *c* if the molecule was appropriately presented to the immune system by polymerization with glutaraldehyde or by coupling to bovine IgG (7), conditions that may circumvent T-cell-mediated tolerance. The antibodies produced against the self antigen appeared to bind in the same region as the antibodies that were previously produced against foreign cyt *c* and, hence, were apparently directed to evolutionarily variable regions (8).

Recent evidence from many laboratories has indicated that synthetic peptides that represent regions within proteins could be used as representative immunogens for those regions (9–13). We constructed two synthetic peptides corresponding to an evolutionarily conserved region that includes the NH_2-terminal tetrapeptide of mammalian cyt *c* to use as probes to identify potential autoantigenic sites within conserved regions of cyt *c*. Both peptides were assessed for their capacity to act as immunogens for the production of anti-self cyt *c* antisera and to bind rabbit anti-rodent cyt *c* antibody. The findings from these studies indicate the existence of an immunogenic determinant in an evolutionarily conserved region of cyt *c* that contains residues 1–4. This determinant can induce anti-self cyt *c* antibodies whether presented as a peptide on a carrier protein or in the context of the intact molecule as polymerized mammalian cyt *c*.

MATERIALS AND METHODS

Native Protein Antigens. Mouse cyt *c* was a gift from Emanuel Margoliash (Northwestern University, Evanston, IL). All other cyt *c* used in this study, including rat cyt *c*, which is identical in sequence to mouse cyt *c* (14), was purchased from Sigma.

Cyt *c* is only weakly immunogenic in monomeric form (15); thus, for immunization it was used either polymerized with 0.1% glutaraldehyde by the method of Reichlin *et al.* (15) or conjugated to the immunogenic carrier protein bovine IgG. Two procedures were used for generating immune responses in rabbits. In one case, a primary immunization of glutaraldehyde-polymerized rat cyt *c* (100 μg) in complete Freund's adjuvant was followed in 3 wk with the same antigen in incomplete Freund's adjuvant. In the other procedure, cyt *c* (100 μg) coupled to bovine IgG with glutaraldehyde (16) was used for the primary immunization followed in 2–3 wk by polymerized cyt *c*.

In antibody assays, the proteins were used as simple solutions of their crystalline monomeric form.

Design and Preparation of Peptide Antigens. Two peptides that correspond to the following segments of rabbit cyt *c*, residues *N*-acetyl-(1–9)-Tyr, with sequence CH_3CO-Gly-Asp-Val-Glu-Lys-Gly-Lys-Lys-Ile-Tyr-OH (peptide A) and residues *N*-acetyl-(1–4)-Gly-(97–100), with sequence CH_3CO-Gly-Asp-Val-Glu-Gly-Tyr-Leu-Lys-Lys-OH (peptide B), were synthesized by Peninsula Laboratories (San Carlos, CA). The composition of the peptides was confirmed by amino acid analysis: peptide A (Gly, 2.04; Asp, 0.96; Val, 0.82; Glu, 0.85; Lys, 3.15; Ile, 0.68; Tyr, 0.78), peptide B (Gly, 2.06; Asp, 0.93; Val, 0.81; Glu, 0.87; Tyr, 1.09; Leu, 1.06, Lys, 2.19). The rationale for the construction of these peptides was as follows: the residues on an antigen encompassed by an antibody-combining site probably depend on (*i*) the size of the site, (*ii*) which residues of the antigen are immunodominant, and (*iii*) the spatial orientation of the antibody relative to the antigen. On examination of the three-dimensional structure of the horse cyt *c* (17), it was deduced that the presentation of the NH_2-terminal residues 1–4 of cyt *c* to the antibody-combining site might involve residues 5–9 or 97–100 depending on the orientation of cyt *c*. Therefore,

The publication costs of this article were defrayed in part by page charge payment. This article must therefore be hereby marked "*advertisement*" in accordance with 18 U.S.C. §1734 solely to indicate this fact.

Abbreviation: cyt *c*, cytochrome *c*.

*To whom reprint requests should be addressed.

we attempted to design peptides that would mimic these two different surface presentations of the potential antigenic site at the NH_2 terminus. Two analogues of these peptides in which a cysteinyl residue was incorporated between the *N*-acetyl end group and the first residue, glycine, were also synthesized for us by Peninsula Laboratories for studies on structural recognition.

To monitor the conjugation of the peptides to carrier proteins for assays and immunization of animals, we used ^{125}I-labeled peptides in analytical trials. The amino acid sequence of cyt *c* contained in the peptide *N*-acetyl-(1–4)-Gly-(97–100) included a tyrosine residue to which the ^{125}I could be covalently attached. Since the first nine residues of cyt *c* do not include tyrosine, it was added to the carboxyl terminal end of peptide 1–9. The NH_2-terminal end of each peptide was blocked with an acetyl group because *N*-acetylation occurs naturally in vertebrate cyt *c* as a post-translational modification (18).

A peptide that represents the common segment in the two peptides described above—i.e., *N*-acetyl-(1–4)—was synthesized by us on a polyamide resin (Chemical Dynamics, South Plainfield, NJ) with a cleavage-resistant sarcosyl-ethylene diamine spacer arm using *N*-α-fluorenylmethyloxycarbonyl amino acid derivatives, tert-butyl side-chain protecting groups for the side-chain carboxylic groups, and standard coupling procedures (19, 20). The *N*-α-fluorenylmethyloxycarbonyl group was cleaved by 20% piperidine between couplings and the NH_2 terminus of the peptide was *N*-acetylated before side-chain deprotection using 10% acetic anhydride and 10% diisopropylethylamine in dimethylformamide. Side-chain protecting groups were cleaved by 2 M HBr in acetic acid/trifluoroacetic acid (1:1) with the fully deprotected peptide remaining attached by its COOH terminus to the resin. The composition of the completed peptide was confirmed by amino acid analysis (Gly, 0.95; Asp, 1.10; Val, 0.89; Glu, 1.14).

Subsequent RIA of this peptide was performed with the peptide still covalently attached to the polyamide resin by the procedure of Smith *et al.* (21). RIAs of the antisera on the polyamide resin alone and on a peptide corresponding to region 41–46 in rodent cyt *c*, which was attached to the resin, were also performed to assess binding that is not antigen specific. Binding of nonspecific antibodies to the peptides was measured with preimmune rabbit immunoglobulin (15 μg/ml) prepared from the antisera of control rabbits by ammonium sulfate fractionation.

Samples of dry peptide/polyamide (1 mg) were swollen and washed 3 times with 0.1 M borate buffer (pH 8.5) containing Tween 20 (0.2%) and NaCl (1 M). Affinity-purified rabbit antibodies from hyperimmune antisera were diluted with this buffer containing 0.5% bovine serum albumin to an antibody concentration of 15 μg/ml. Antibody binding was detected with ^{125}I-labeled goat anti-rabbit IgG.

In addition to the synthetic peptide antigens described above the three major cyanogen bromide-cleaved fragments of mouse cyt *c*—namely, residues 1–65, 66–80, and 81–104—were prepared from the native protein as described (22).

Coupling the Peptide to Carriers. The synthetic peptides used were coupled to polypeptide carriers. For assay purposes, the carriers were bovine serum albumin (Sigma) and poly-L-lysine (M_r, ≈260,000; Sigma) and for immunization purposes bovine IgG (Pentex, FII, Miles) was the carrier protein.

To couple the peptides to carriers using 0.1% glutaraldehyde, carrier (5 mg) and peptide (1 mg) were dissolved in 1 ml of 0.1 M ammonium acetate (pH 7.0). Glutaraldehyde was added slowly with stirring to a final concentration of 0.1% and was allowed to react for 2 hr at room temperature. The reactants and products were separated by dialysis; in some experiments, further purification by chromatography with Sephadex G-100 was necessary. Using ^{125}I-labeled peptides as a tracer, we determined that the efficiency of coupling for both peptides was 20%–30% and 5–10 molecules of each peptide were coupled to each carrier molecule.

New Zealand Red rabbits were primed and given booster injections with 375 μg of the peptide–protein conjugate by injection into positions along the back intradermally and in the hind footpads. The primary dose was an emulsification in complete Freund's adjuvant, and the secondary dose was given in incomplete Freund's adjuvant; animals were bled 2–4 wk later.

Solid-Phase Antibody Binding Assays. Antisera were examined for antigenic specificity using ELISA (23) and solid-phase RIA (24). Antisera were incubated on antigen-coated 96-well plates at various dilutions. The plates were developed using goat anti-rabbit IgG, which was either conjugated to horseradish peroxidase (ELISA) or labeled with ^{125}I (RIA). To determine whether antisera contained different antibody populations specific for each peptide antigen, antisera were preincubated on a plate coated with one peptide, and unbound material was then assayed for binding to the other peptide by the procedure described above. In some experiments, the antibodies were purified prior to assay by affinity chromatography on rodent cyt *c* covalently coupled to cyanogen bromide-activated Sepharose 4B (25).

Antibody titers were determined using either an RIA or ELISA. The principles of these assays are identical except for the detecting signals. The antigens used to assess antibody binding were rat cyt *c* and the two peptides representative of the NH_2 terminus of cyt *c* coupled to carrier polypeptides. To measure nonspecific binding, the carrier polypeptide alone and bovine serum albumin were used. As an index of the reactivity of each antiserum, the ratio of the binding of antibodies to each peptide over its binding to cyt *c* was calculated as follows:

$$\% \text{ reactivity} = \frac{\text{cpm bound to peptide on carrier} - \text{cpm bound to carrier}}{\text{cpm bound to cyt } c - \text{cpm bound to bovine serum albumin}}$$

The values used in this calculation were taken at serum dilutions at which antibody bound was not saturating.

RESULTS

The Immunogenicity of a Peptide Including Residues 1–4 of Mammalian cyt *c*. Serum from a New Zealand Red rabbit immunized with peptide *N*-acetyl-(1–4)-Gly-(97–100) coupled to bovine IgG was tested by both ELISA and RIA for binding to both the homologous peptide and the peptide *N*-acetyl-(1–9)-Tyr, each coupled to polylysine, as well as to intact mammalian cyt *c*. The results of such an assay using affinity-purified antibodies on the peptides are shown in Fig. 1. It can be seen that this antiserum contained antibodies that bound to the homologous peptide *N*-acetyl-(1–4)-Gly-(97–100) and to the peptide *N*-acetyl-(1–9)-Tyr. The antisera induced by peptide *N*-acetyl-(1–4)-Gly-(97–100) also included antibodies that bound to intact rodent cyt *c* (Fig. 2). Thus, it appears that immunization of rabbits with a peptide including the first four residues of mammalian cyt *c* can give rise to antibodies that bind to a region of the molecule evolutionarily conserved throughout mammalian species (26) and heretofore believed to be immunologically silent.

To provide further evidence for this specificity, solid-phase RIAs were carried out with antibodies affinity purified on mouse cyt *c*. A variety of species variant cytochromes and synthetic peptides coupled to polylysine were used as

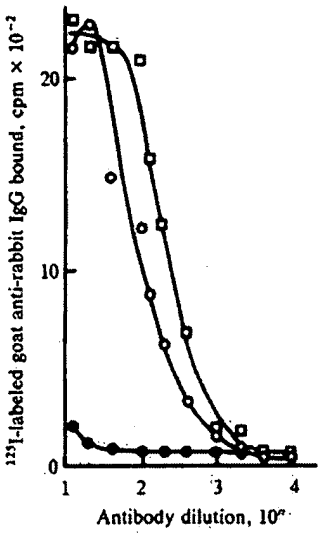

FIG. 1. RIA of affinity-purified antibodies to *N*-acetyl-(1–4)-Gly-(97–100) coupled to bovine IgG on *N*-acetyl-(1–4)-Gly-(97–100)-polylysine (□), *N*-acetyl-(1–9)-Tyr-polylysine (○), or polylysine (●).

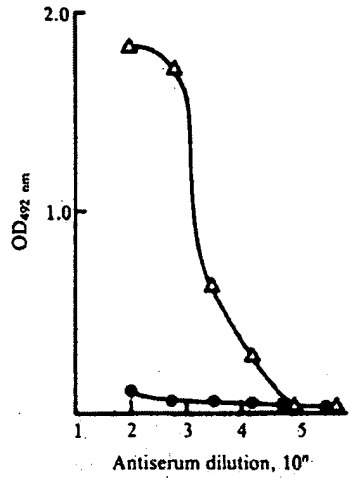

FIG. 2. ELISA of rabbit antisera to *N*-acetyl-(1–4)-Gly-(97–100) coupled to bovine IgG on mouse cyt *c* (△) or bovine serum albumin (●).

antigens (Fig. 3). The antibodies cross-reacted with a panel of cyt *c* from various mammalian sources, all of which are *N*-acetylated and are homologous for residues 1–4. There is little reactivity to two cyt *c* from the yeasts *Saccharomyces* and *Candida* (Fig. 3*a*), which are not acetylated and have little homology in this region (26). The reactivity of the antibody to tuna cyt *c*, in which alanine replaces glutamic acid at residue 4 in the molecule, is significantly lower than to the other vertebrate cytochromes; however, the avian cytochromes, which also have one amino acid substitution in this region (isoleucine replaces valine at position 3), show complete reactivity to antibodies to *N*-acetyl-(1–4)-Gly-(97–100).

The binding of the antibodies to *N*-acetyl-(1–9)-Tyr and *N*-acetyl-(1–4)-Gly-(97–100) could be blocked by incorporating a cysteinyl residue in the peptide between the *N*-acetyl end group and glycine, the first residue (Fig. 3*b*). In addition, preadsorption by either peptide removed the population of antibodies available for binding to the other peptide (Fig. 3*b*). This indicates that the specificity of these antibodies resides in the common four residues of these peptides—i.e., *N*-acetyl-(1–4). That these antibodies can in fact bind to a peptide of this length was confirmed by synthesizing this peptide on a polyamide resin by the method described in *Materials and Methods*, which enables the peptide to be assayed while still attached to the solid-phase resin (21). Fig. 3*c* shows antibody specifically bound to the peptide *N*-acetyl-(1–4) attached to resin compared to nonspecific binding to the resin alone. Nonspecific binding to control peptide representing region 41–46 in cyt *c* showed similar levels to the polyamide control (results not shown). Nonspecific rabbit antibodies showed no significant binding to either the resin or the resin-attached peptides.

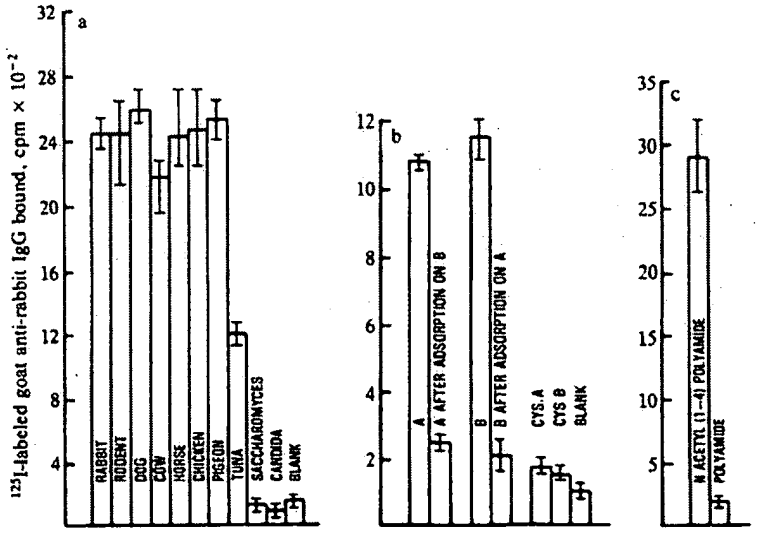

FIG. 3. RIA of affinity-purified rabbit anti-*N*-acetyl-(1–4)-Gly-(97–100) on different panels of antigens. Values shown were obtained from dilutions of antibody preparations that gave less than saturated binding. (*a*) Eukaryotic cyt *c*. (*b*) Synthetic peptides coupled to polylysine. A, *N*-acetyl-(1–9)-Tyr-polylysine; B, *N*-acetyl-(1–4)-Gly-(97–100)-polylysine; Cys A, *N*-acetyl-Cys-(1–9)-Tyr-polylysine; Cys B, *N*-acetyl-Cys-(1–4)-Gly-(97–100)-polylysine; blank, polylysine. (*c*) Synthetic peptide *N*-acetyl-(1–4) covalently attached to a polyamide resin through its COOH terminus.

Table 1. Reactivity with NH_2-terminal peptides of four rabbit antisera to polymerized mouse cyt *c*

Antiserum	% reactivity with peptides	
	N-acetyl-(1–9)-Tyr	*N*-acetyl-(1–4)-Gly-(97–100)
1	91	95
2	72	67
3	69	49
4	8	5

Antiserum 1: First immunization and booster injection was glutaraldehyde-polymerized mouse cyt *c*. Antisera 2 and 3: First immunization was glutaraldehyde-polymerized conjugate of bovine IgG and mouse cyt *c*; booster injection was glutaraldehyde-polymerized mouse cyt *c*. Antiserum 4: Obtained from Urbanski and Margoliash (3); soluble fraction from glutaraldehyde-polymerized mouse cyt *c* used for immunization.

That antibodies to *N*-acetyl-(1–4)-Gly-(97–100) were specific for the first four residues of the peptide was further demonstrated by removing all reactivity to cyt *c* and peptides *N*-acetyl-(1–4)-Gly-(97–100) and *N*-acetyl-(1–9)-Tyr by preadsorption on *N*-acetyl-(1–4) covalently bound to the polyamide resin. Adsorption of the antibodies by polyamide resin alone or control peptide 41–46 had no effect on the reactivity of the antibodies to these antigens.

It should be noted that a rabbit immunized with peptide *N*-acetyl-(1–9)-Tyr coupled to bovine IgG produced antibodies that were strongly reactive with peptide *N*-acetyl-(1–9)-Tyr but were weakly reactive with the peptide *N*-acetyl-(1–4)-Gly-(97–100) and not reactive at all with intact mouse cyt *c* (results not shown).

Antibodies to Polymerized Rodent cyt *c* Are Reactive with Residues 1–4. The above findings demonstrate not only that a peptide displaying a self antigenic determinant could be immunogenic, but also that such a peptide could be an excellent probe for detecting the presence within an antiserum of an antibody population to a given region of a protein. We therefore examined several antisera generated in rabbits by immunization with various forms of rodent cyt *c* to determine whether antibodies to the region of 1–4 were present but heretofore undetected. We generated antisera from three rabbits: one by immunization with polymerized rat cyt *c* and two by a primary immunization with rat cyt *c* coupled to bovine IgG followed by immunization with polymerized cyt *c*. The fourth antiserum was obtained from E. Margoliash and was one of the antisera previously tested by Urbanski and Margoliash for reactivity to regions of cyt *c* (3). All four antisera contained reactivity to both peptides and the reactivities to the peptides of antisera 1, 2, and 3 (raised in this laboratory) are considerably greater than that of antiserum 4 (prepared by Urbanski and Margoliash) (Table 1). This is possibly due to differences in the immunization procedures used in the two studies. Although polymerized cyt *c* was used both by us and by Urbanski and Margoliash, a much larger quantity of immunogen (5 mg) was used for each immunization in the latter study (3). In addition, the degree of aggregation of cyt *c* used in our work was much greater; indeed, our immunogen contained particulate material, whereas the other workers used only soluble complexes for immunization. It is likely that polymerization causes alterations in the polypeptide that could result in changes within potentially immunogenic determinants. In addition, New Zealand Red rabbits were used in our study, whereas New Zealand White rabbits were used by Urbanski and Margoliash.

The recognition of the NH_2 terminus by the antisera raised in our laboratories was further delineated by assessing binding to various antigens. The results obtained for all three antisera were similar and are exemplified in Fig. 4, which represents the analyses of antiserum 1 (Table 1). It can be seen that these antibodies recognize all tested vertebrate cytochromes, which are identical at the NH_2 terminus but do not recognize yeast cytochromes, which have considerably different NH_2 termini (26) (Fig. 4*a*). Furthermore, the anti-

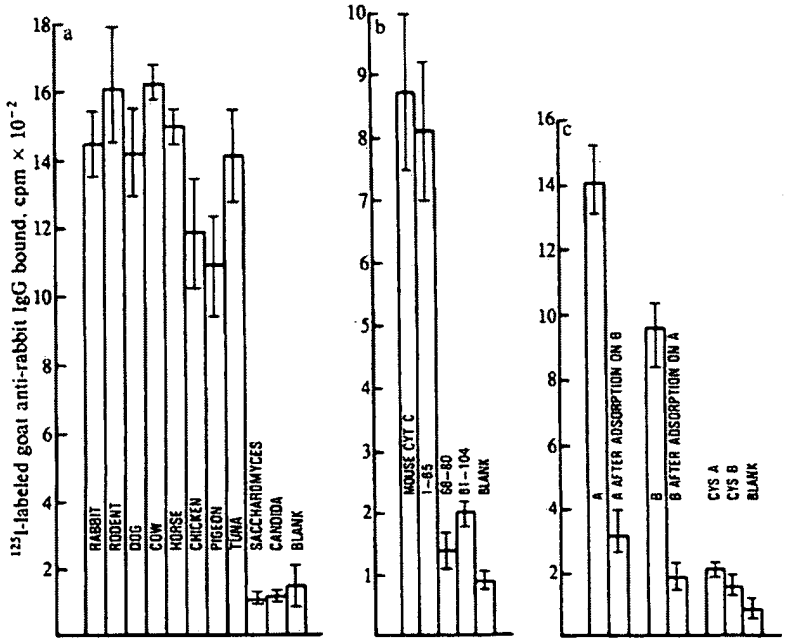

FIG. 4. RIA of rabbit antiserum (antiserum 1 in Table 1) to polymerized rat cyt *c* on different panels of antigens. Values were obtained from dilutions of antibody preparations that gave less than saturated binding. (*a*) Eukaryotic cyt *c*. (*b*) Antigens coupled to polylysine. Mouse cyt *c*, CNBr-cleaved fragments from mouse cyt *c* 1–65, 66–80, 81–104, and polylysine control (blank). (*c*) Synthetic peptides coupled to polylysine. A, *N*-acetyl-(1–9)-Tyr-polylysine; B, *N*-acetyl-(1–4)-Gly-(97–100)-polylysine; Cys A, *N*-acetyl-Cys-(1–9)-polylysine; Cys B, *N*-acetyl-Cys-(1–4)-Gly-(97–100)-polylysine; blank, polylysine.

genicity is predominantly located in the region of residues 1–65 shown by the binding of the antibodies to cyanogen bromide-cleaved fragments of cyt *c*, each of which are coupled to polylysine to ensure that the peptides bind equally well to the plates (Fig. 4*b*). Finally, the reactivity can be isolated to residues 1–4 because preadsorption of the antibody on either peptide removes the reactivity of the anti-cyt *c* antibodies to the other peptide (Fig. 4*c*), and the inclusion of a cysteinyl residue between the *N*-acetyl end group and residue 1 in both *N*-acetyl-(1–9)-Tyr and *N*-acetyl-(1–4)-Gly-(97–100) blocks binding (Fig. 4*c*).

DISCUSSION

In this study, we have used synthetic peptides representative of the NH_2-terminal sequence of mammalian cyt *c* to ask directly whether mammals can respond to an evolutionarily conserved region of a protein. The results indicate that one such peptide can elicit antibodies in rabbits that recognize not only the immunizing peptide but two other peptides that contain the same four NH_2-terminal residues as well as native rabbit cyt *c*. Furthermore, these peptides were used to show that antisera raised in rabbits immunized with rodent cyt *c* include antibodies against this evolutionarily conserved region. The levels of this population of antibodies vary among different antisera and may depend on the strain of rabbit used and the degree of aggregation of cyt *c* used for immunization.

The NH_2-terminal region of mammalian cyt *c* represents not only a highly conserved region of a mammalian protein but also a region that heretofore had been thought to be nonimmunogenic. It should be noted, however, that reactivity to this region of cyt *c* may arise from circumstances that are consistent with the hypothesis that conserved regions of proteins are not, in general, immunogenic (8). The immunogenicity of mouse cyt *c* has been shown to involve residues 44, 62, and 89 (3). The NH_2 terminus of the cytochrome molecule is in topographic proximity to one of these immunodominant residues—in fact, residue 1 is ≈6 Å from residue 89. What we may be detecting, therefore, with synthetic peptide *N*-acetyl-(1–4) are antibodies to a topographic determinant on the intact protein that includes both the NH_2-terminal region and residue 89. Such a situation is thought to occur with myoglobin where surface residues, which are remote in sequence from the short contiguous sequences originally proposed by Atassi as representing the total antigenicity of the molecule (27), have been clearly identified as being involved in the antigenic sites of this protein (28). If this is the case, the primary response to this determinant on polymerized cyt *c* may, in fact, be stimulated by the evolutionarily variant residue 89.

It is also possible that the chemical reaction of polymerization required for increasing immune responses to cyt *c* may cause disturbances in polypeptide folding, which then trigger an antibody response. The NH_2-terminal segment of cyt *c* may be more susceptible to this kind of conformational alteration than other regions of the molecule, possibly allowing for breaking of tolerance at the B-cell level. Alternatively, tolerance at the T-cell level could be broken through conformational alteration of T-cell determinants at other sites on cyt *c*, in which case the relative immunogenicity of the first few residues may be a consequence of their presentation as an exposed terminus that is available for "end on" recognition by the immunoglobulin receptor on B cells. Such recognition has previously been found to be important in antibody binding for carbohydrates (29). Evidence for this view is provided by the observation that none of the antibodies that recognize the NH_2 terminus of cyt *c* binds to the peptides extended by an NH_2-terminal cysteinyl residue. Such an addition would be expected to markedly affect end on recognition but to interfere less with recognition of determinants within the peptide sequence.

The studies presented here not only confirm the work of many others in demonstrating the utility of synthetic peptides for the study of the immunogenicity of defined regions of proteins but also extend this approach to the analysis of potential reactivities to self determinants.

It is clear that further studies using synthetic peptides constructed of regions that are conserved in contrast to those that are not conserved both as immunogens and as assay probes for antibodies against intact molecules will be highly useful in elucidating heretofore undetected antigenic regions in proteins.

This work was supported by Grants AI 19499 and AI 15797 from the National Institutes of Health. R.J. was the recipient of a Damon Runyon/Walter Winchell Fellowship for Cancer Research. P.R.M. is the recipient of a fellowship from the Arthritis Foundation.

1. Reichlin, M. (1975) *Adv. Immunol.* **20**, 71–123.
2. Burnet, F. M. (1975) *Aust. J. Sci.* **20**, 67–69.
3. Urbanski, G. J. & Margoliash, E. (1977) *J. Immunol.* **118**, 1170–1180.
4. Jemmerson, R. & Margoliash, E. (1979) *J. Biol. Chem.* **254**, 12706–12716.
5. Eng, J. & Reichlin, M. (1979) *Mol. Immunol.* **16**, 225–230.
6. Berman, P. W. & Harbury, H. A. (1980) *J. Biol. Chem.* **255**, 6133–6137.
7. Nisonoff, A., Margoliash, E. & Reichlin, M. (1967) *Science* **155**, 1273–1275.
8. Jemmerson, R. & Margoliash, E. (1979) *Nature (London)* **282**, 468–471.
9. Arnon, R. (1980) *Annu. Rev. Microbiol.* **34**, 593–618.
10. Walter, G., Scheidtmann, K.-H., Carbone, A., Laudano, A. P. & Doolittle, R. F. (1980) *Proc. Natl. Acad. Sci. USA* **77**, 5197–5200.
11. Audibert, F., Jolivet, M., Chedid, L., Alouf, J. E., Boquet, P., Rivaille, P. & Siffert, O. (1981) *Nature (London)* **289**, 593–594.
12. Baron, M. H. & Baltimore, D. (1982) *J. Virol.* **43**, 969–978.
13. Lerner, R. (1982) *Nature (London)* **299**, 592–596.
14. Carlson, S. S., Mross, G. A., Wilson, A. C., Mead, R. T., Wolin, L. D., Bowers, S. F., Foley, N. T., Muijsers, A. O. & Margoliash, E. (1977) *Biochemistry* **16**, 1437–1442.
15. Reichlin, M., Nisonoff, A. & Margoliash, E. (1970) *J. Biol. Chem.* **245**, 947–954.
16. Reichlin, M. (1980) *Methods Enzymol.* **70**, 159–165.
17. Dickerson, R. E. (1972) *Sci. Am.* **226** (4), 58–72.
18. Margoliash, E. (1972) *Harvey Lect.* **66**, 177–247.
19. Arshady, R., Atherton, E., Clive, D. L. J. & Sheppard, R. C. (1981) *J. Chem. Soc. Perkin Trans. 1*, 529–537.
20. Atherton, E., Logan, C. J. & Sheppard, R. C. (1981) *J. Chem. Soc. Perkin Trans 1*, 538–546.
21. Smith, J. A., Hurrell, J. G. & Leach, S. J. (1977) *Immunochemistry* **14**, 565–568.
22. Corradin, G. & Harbury, H. A. (1970) *Biochim. Biophys. Acta* **221**, 489–496.
23. Engvall, E. (1980) *Methods Enzymol.* **70**, 419–439.
24. Pierce, S. K. & Klinman, N. K. (1977) *J. Exp. Med.* **146**, 509–519.
25. Jemmerson, R. & Margoliash, E. (1980) *Methods Enzymol.* **70**, 244–262.
26. Borden, D. & Margoliash, E. (1976) in *Handbook of Biochemistry and Molecular Biology*, ed. Fasman, G. D. (The Chemical Rubber Co., Cleveland, OH), Vol. 3, pp. 268–279.
27. Atassi, M. Z. (1975) *Immunochemistry* **12**, 423–438.
28. Benjamin, D. C., Berzofsky, J. A., East, I. J., Gurd, F. R. N., Hannum, C., Leach, S. J., Margoliash, E., Michael, J. G., Miller, A., Prager, E. M., Reichlin, M., Sercaz, E. E., Smith-Gill, S. J., Todd, P. E. & Wilson, A. C. (1984) *Annu. Rev. Immunol.* **2**, 67–101.
29. Kabat, E. A. (1966) *J. Immunol.* **97**, 1–11.

nature immunology

EXHIBIT E

Structure of and influence of a tick complement inhibitor on human complement component 5

Folmer Fredslund[1], Nick S Laursen[1], Pietro Roversi[2], Lasse Jenner[1,7], Cristiano L P Oliveira[3,4], Jan S Pedersen[3,4], Miles A Nunn[5], Susan M Lea[2], Richard Discipio[6], Lars Sottrup-Jensen[1] & Gregers R Andersen[1,4]

To provide insight into the structural and functional properties of human complement component 5 (C5), we determined its crystal structure at a resolution of 3.1 Å. The core of C5 adopted a structure resembling that of C3, with the domain arrangement at the position corresponding to the C3 thioester being very well conserved. However, in contrast to C3, the convertase cleavage site in C5 was ordered and the C345C domain flexibly attached to the core of C5. Binding of the tick C5 inhibitor OmCI to C5 resulted in stabilization of the global conformation of C5 but did not block the convertase cleavage site. The structure of C5 may render possible a structure-based approach for the design of new selective complement inhibitors.

Human C5 is a 196-kilodalton protein that is pivotal in the complement system and is cleaved by the C5 convertase to the small anaphylatoxin C5a (residues 678–751) and the large C5b fragment. The binding of C5a to the G protein–coupled receptor C5aR triggers intracellular signaling, which results in chemotaxis, a respiratory burst and release of proinflammatory mediators from granulocytes[1,2]. In addition to C5aR, C5a can also be recognized by the homologous C5L2 receptor, a nonsignaling receptor for C5a. The function of C5L2 is enigmatic, as it has been ascribed both an anti-inflammatory function[3] as well as a function in promoting inflammatory responses to C5a *in vivo*[4]. The C5b fragment first combines with the C6 protein and then with the C7 protein to initiate the formation of the membrane attack complex (MAC) in the membrane of invading microorganisms[5]. The C5bC6C7 complex can integrate into phospholipid membranes, but transmembrane channels are first formed when the C8 protein joins the complex[6]; the resulting C5bC6C7C8 intermediate initiates C9 circular polymerization[7]. The final assembly consists of either a monomer or dimer of C5bC6C7C8 with 10–18 subunits of C9 arranged in a transmembrane tubular structure, creating a hole about 100 Å in diameter[8].

Human C5 is specifically cleaved at Arg751-Leu752 by the classical pathway C3 convertase C4bC2a or by the alternative pathway convertase C3bPBb; however, these convertases cleave C5 efficiently only if an additional C3b molecule is deposited covalently on the convertases[9–11] to form either C3bC4bC2a or $(C3b)_2PBb$. OmCI is a 17-kilodalton protein from the soft tick *Ornithodoros moubata* that binds directly and tightly to C5 (ref. 12) and prevents convertase cleavage of C5 into C5b and C5a. Recombinant OmCI is a likely candidate as a complement inhibitor[13]. The development of C5-specific inhibitors is desirable, as only the terminal complement components would be affected, whereas the beneficial immunoprotective and immunoregulatory effects mediated by 'upstream' complement components would remain functional[14,15].

C5 is homologous to the complement proteins C3 and C4 and other proteins of the α_2-macroglobulin (α_2M) 'superfamily' but does not contain an internal Cys-Gln thioester bond[16]. The structures of C5a and the carboxy-terminal C345C domain of C5 have been determined by nuclear magnetic resonance[17,18]. The structures of human C3 (ref. 19) and bovine C3 (ref. 20) suggest that all members of the α_2M superfamily would have a similar architecture. However, as the shielding of the thioester from water in C3 seems to be the main organizing principle for the α-chain of C3 and presumably other thioester-containing proteins in the family, the structure of C5 could be somewhat different from that of C3 and unique in the family. The structure of the insect thioester protein TEP[21] has shown that the arrangement of the MG1-MG6 domains can be very different from that of C3 (refs. 19,20) or C3b[22,23]. To provide an accurate structural basis for delineating the functional and structural features of C5, we present here the crystal structure of C5 together with a solution scattering–based model of the C5-OmCI complex. Our results offer a molecular 'scaffold' for the rational design of C5-specific inhibitors aimed at preventing undesired complement responses in a variety of disease conditions and after organ transplantation.

[1]Department of Molecular Biology, University of Aarhus, DK-8000 Aarhus, Denmark. [2]Sir William Dunn School of Pathology, University of Oxford, Oxford OX1 3ER, UK. [3]Department of Chemistry, University of Aarhus, DK-8000 Aarhus, Denmark. [4]Centre for mRNP Biogenesis and Metabolism, University of Aarhus, Denmark. [5]Centre for Ecology and Hydrology Oxford, Oxford OX1 3SR, UK. [6]La Jolla Institute for Experimental Medicine, 505 Coast Boulevard S., La Jolla, California 92037, USA. [7]Present address: Institut de Génétique et de Biologie Moléculaire et Cellulaire, Illkirch 67404, France. Correspondence should be addressed to G.R.A. (gra@mb.au.dk).

Received 11 March; accepted 21 May; published online 8 June 2008; corrected after print 20 June 2008; doi:10.1038/ni.1625

Table 1 Data collection and refinement

	Native	Native	$Sm(Acetate)_2$	$GdSO_4$	NaI
Data collection					
Space group	$P3_1$	$P3_121$	$P3_121$	$P3_121$	$P3_121$
Cell dimensions					
a, *c* (Å)	144.3, 241.0	144.3, 241.0	143.8, 244.6	144.6, 242.5	144.2, 240.9
Resolution (Å)	30–3.1	30–3.1	50–4.6	50–4.6	50–4.5
	(3.21–3.1)	(3.21–3.1)	(4.8–4.6)	(4.8–4.6)	(4.8–4.5)
R_{sym}	0.040	0.049	0.106	0.122	0.155
	(0.574)	(0.648)	(0.237)	(0.353)	(0.48)
I / σI	13.5 (1.3)	18.1 (1.8)	9.4 (4.4)	10 (2.9)	7.2 (2.2)
Completeness (%)	96.9 (85.6)	98.3 (89.0)	77.2 (74.3)	99.6 (100)	94.7 (96.6)
Redundancy	1.4 (1.1)	3.2 (2.9)	2.6 (2.7)	2.6 (2.6)	2.2 (2.1)
Refinement statistics					
Resolution (Å)	30–3.1				
Reflections	98,570				
R_{work}/R_{free}	23.6/28.1				
Atoms					
Protein	24,656				
Ligand / ion	87				
B-factors					
Protein	140.6				
Ligand / ion	250.3				
r.m.s.d.					
Bond lengths (Å)	0.004				
Bond angles (°)	0.846				

For the derivatives, Friedel pairs were kept separated. One crystal was used for all data sets. Values in parentheses are for the shell of highest resolution. $Sm(Acetate)_2$, $GdSO_4$ and NaI are the samarium, gadolinium and iodide derivatives, respectively.

RESULTS

The crystal structure of C5

We determined the crystal structure of human C5 with a combination of anomalous data from three heavy-atom derivatives and molecular replacement (**Table 1** and **Supplementary Fig. 1** online). Like C3 and TEP, C5 contains eight MG domains (MG1–MG8), a CUB domain, the C5d domain (structurally homologous to the thioester-containing TE domain in C3 and TEP), the C5a domain (also called 'anaphylatoxin', not present in TEP) and an extended linker region packed between MG1–MG2 and MG4–MG6 (**Fig. 1** and **Supplementary Fig. 2** online). The linker and C5a form a continuous insert in the MG6 domain, whereas C5d is inserted in the CUB domain. The MG1–MG6 domains are arranged into a right-handed 'superhelix', whereas CUB, C5d and MG8 pack tightly into a 'superdomain' (**Fig. 1b–d**). The MG1–MG6 superhelix is connected with the CUB-C5d-MG8 superdomain through the MG7 domain, and C5a, located between MG3 and MG8, acts as a molecular wedge between the two structural blocks. We traced all residues between Glu20 and Cys1676 (prepro-C5 numbering used throughout; a value of 18 should be subtracted for numbering of mature C5) except for the loop regions 744–748, 872–881 and 1387–1398. There are two molecules of C5 in the asymmetric unit and in one of these, C5-1, the C345C domain is placed on a pseudo-twofold noncrystallographic symmetry axis (**Supplementary Fig. 1b**), which almost perfectly relates the two copies of the C5 core, residues 20–1515, to each other. Here it contacts the MG7 domain and comes near loop regions in C5a, the MG8 and the MG3 domains (**Fig. 1a**). In the second C5 molecule in the crystal, C5-2, weak residual density suggests that the C345C domain is located in a way more similar to its placement in C3. Indeed, we obtained a molecular-replacement solution that positioned the C345C domain in the crystal lattice in a C3-like placement and also satisfied the disulfide bridge Cys1532-Cys1606. However, only weak scattered density was present for the domain, and therefore the C345C domain of C5-2 is not included in the structure deposited at the protein data bank of the Research Collaboratory for Structural Bioinformatics. A flexibly attached C345C domain in C5 is supported by our biophysical data (discussed below) and, despite being traceable, the C345C domain is also relatively mobile in the structures of C3, C3c and C3b[19,20,22,23]. The C345C domain and the MG8 domain are linked by the anchor region 1516–1532. The C345C domain is also linked by the anchor region to the MG7 domain through two disulfide bridges (Cys1527-Cys866 and Cys1532-Cys1606; **Supplementary Fig. 1c**). The C5-1 helix containing residues 1522-1531 swivels by roughly 180° around the Cys1527-Cys866 disulfide bridge to accommodate the altered orientation of the C345C domain in C5-1 relative to that of C5-2 and C3.

By comparing C3, TEP and C5, it became evident that these molecules have two main structural units. The first main unit is the MG1-6 superhelix; by comparison of C5 and bovine C3, 307 common C_α atom positions overlay with a r.m.s.d. of 1.88 Å (**Fig. 1b**). In TEP, these domains have a much more open arrangement[21], as MG3 compensates for the absence of the anaphylatoxin by interacting extensively with the MG7 and MG8 domains (**Fig. 1c**). The second main structural unit is the CUB-C5d-MG8 superdomain, which has very similar packing in C5, C3 and TEP (**Fig. 1d**). In this superdomain, 418 or 347 C_α positions superimpose with r.s.m.d. values of 1.54 Å or 1.80 Å by comparison of C3 with C5 or of TEP with C5, respectively. However, we noted a rotation of 9° of the MG1-6 superhelix relative to the CUB-C5d-MG8 superdomain in C5 compared with C3, but the MG2 domain seemed to maintain its interface with the C5d domain as in C3 and TEP. In summary, except for the C345C domain, the global architecture of C5 is similar to that of native C3 (refs. 19,20), as suggested before by neutron scattering[24].

The C5d-MG8 domain interface

Our C5 structure showed in atomic detail that the thioester is not a prerequisite for a C3-like MG8-thioester domain interaction. In human C5, Ser1007 and Ala1010 correspond to the thioester-forming cysteine and glutamine residues, respectively, in C3 and other thioester proteins. Despite the absence of the thioester in C5, the interaction of the MG8 domain with residues 1007–1010 in C5d was unexpectedly similar to the equivalent packing of the MG8 and thioester domains in C3 and TEP (**Fig. 2**). In the two thioester-containing proteins, highly conserved residues from the two domains ensure a solvent-excluded environment for the thioester[19–21]. In C3, the water-free environment protects the molecule from hydrolysis before activation by the C3 convertase, which releases C3a and induces a substantial conformational rearrangement[19,22,23,25]. On the basis of sequence conservation, it has been suggested that a similar arrangement of the thioester and the MG8 domains would apply to all proteins of the α_2M superfamily[19,20]. The idea that this domain-packing arrangement

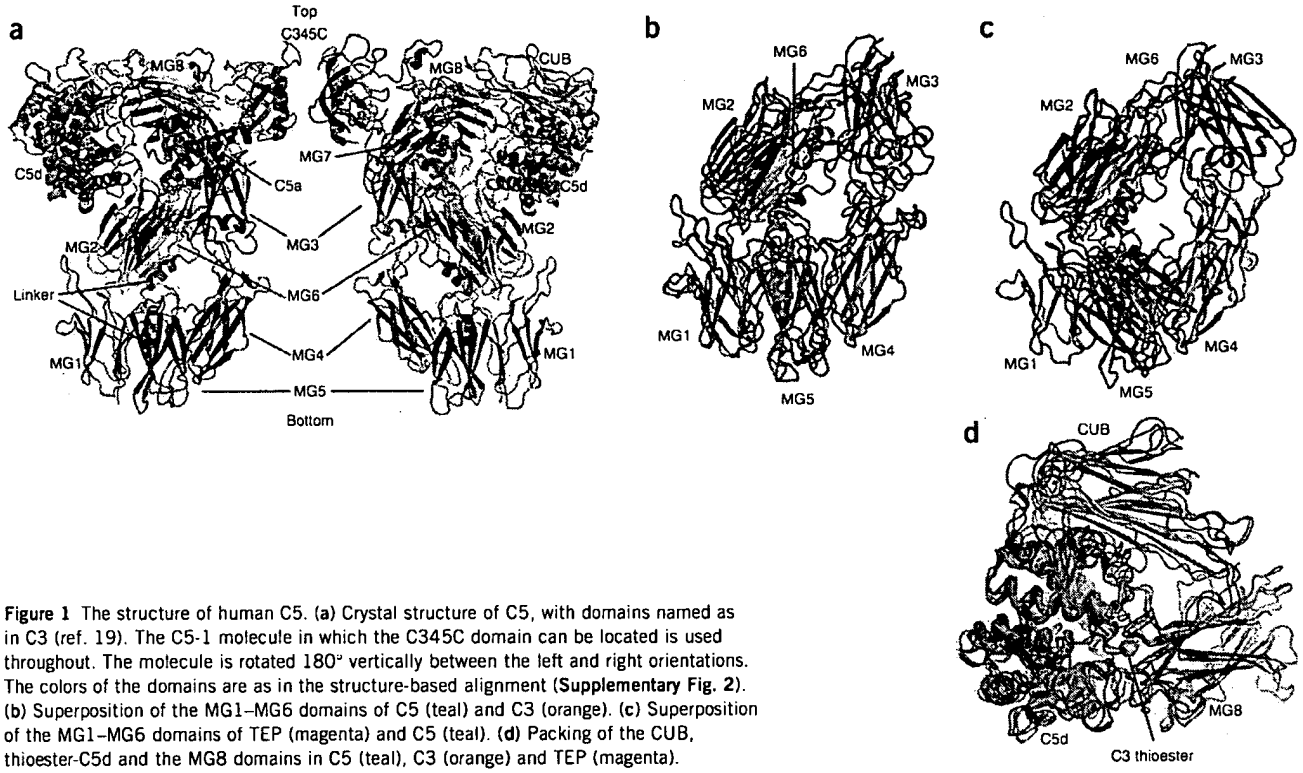

Figure 1 The structure of human C5. (**a**) Crystal structure of C5, with domains named as in C3 (ref. 19). The C5-1 molecule in which the C345C domain can be located is used throughout. The molecule is rotated 180° vertically between the left and right orientations. The colors of the domains are as in the structure-based alignment (**Supplementary Fig. 2**). (**b**) Superposition of the MG1–MG6 domains of C5 (teal) and C3 (orange). (**c**) Superposition of the MG1–MG6 domains of TEP (magenta) and C5 (teal). (**d**) Packing of the CUB, thioester-C5d and the MG8 domains in C5 (teal), C3 (orange) and TEP (magenta).

could be thioester independent has also been indicated by the native-like conformation of a mutant C3 unable to form the thioester, but C4 made mutant in the same way does not attain such a conformation[26].

However, important differences between C3 and C5 are evident, probably caused by the less stringent requirements for a water-free environment in C5. Despite the very similar architecture of the two molecules, the domain interfaces between the thioester-C5d and MG8 domains with the rest of the molecule are much more hydrophobic in C3 than in C5, although the buried surface areas are similar (**Supplementary Table 1** online). Of special interest are three residues in C3 and TEP that pack together and directly face the thioester linkage (**Fig. 2**). These form a hydrophobic 'plug' separating two components in thioester cleavage: C3-Tyr1445 and TEP-Tyr1252 face bulk water, whereas C3-Tyr1481 and TEP-Tyr1287 prevent the catalytic C3-His1125 and TEP-His951 from moving toward the thioester. Between these two flanking residues, C3-Met1399 and TEP-Met1210 directly face the thioester. With very few exceptions, these three residues are strictly conserved in all the thioester-containing proteins but not in C5. As there is no thioester to protect in C5, these residues are replaced by Gln1463, His1421 and His1499 from the MG8 domain, which are the equivalents of C3-Tyr1445 and TEP-Tyr1252, C3-Met1399 and TEP-Met1210, and C3-Tyr1481 and TEP-Tyr1287, respectively. Overall, the high conservation of this domain interface in C3, TEP and C5 even in the absence of thioester suggests that all proteins of the α_2M superfamily adopt a very similar domain interface.

The anaphylatoxin and the convertase binding site

In both C3 (refs. 19,20) and C5, the anaphylatoxin is folded into a four-helix bundle packed between the MG3 domain, the MG8 domain and the future α′-chain 'downstream' of the convertase cleavage site (**Fig. 3a,b**). In human C5, the loop between helices 2 and 3 contains the only unpaired but nonconserved cysteine of C5 (residue 704) and interacts with MG8 and the later C5b α′-chain. A genetic screen of the C5a receptor has shown that this cysteine is juxtaposed with residues 24–30 in the amino-terminal extracellular part of C5aR and, on the basis of additional disulfide bridges between mutant C5a and C5aR, a model for the C5a-C5aR complex has been suggested[27]. Notably, the proposed receptor interface of C5a is similar to the regions interacting with MG3, the α′-chain and MG8 (**Fig. 3c**), although these regions

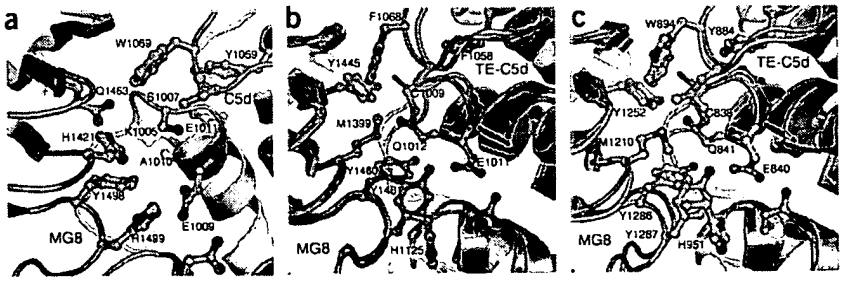

Figure 2 The C5d-MG8 domain interfaces in C5 and the corresponding interface in C3 and TEP. (**a**) Packing of the MG8 (green) and the C5d (gray) domains in C5 around Ser1007 and Ala1010. (**b**) The region in a at the thioester (TE) formed by Cys1009 and Gln1012 in bovine C3 (orange) superimposed onto the C5d domain of C5 (green and gray, as in a). (**c**) The thioester formed by Cys838 and Gln841 in TEP (light blue) and in C5 (green and gray). In b and c, the catalytic histidine residues 1125 and 951 are in the foreground.

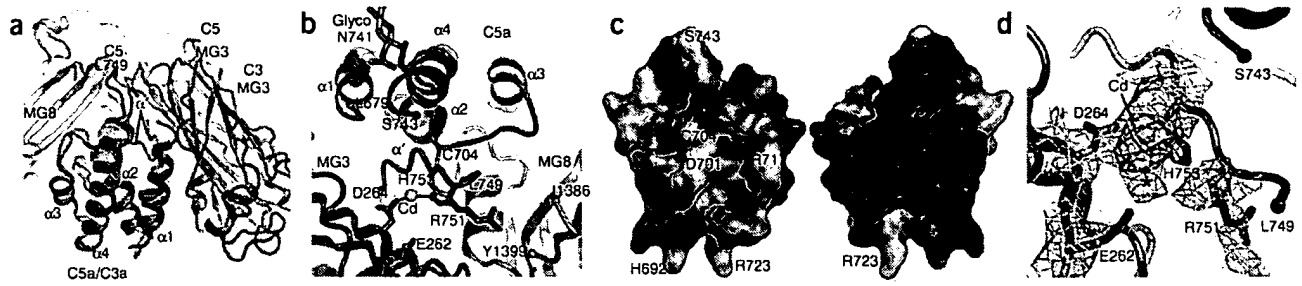

Figure 3 The C5a anaphylatoxin in C5. (a) Accessibility of the convertase site in C5 (teal) and C3 (orange), influenced by packing between C5a and the MG3 domain. (b) Packing of C5a (red) with the future amino-terminal end of the C5b α'-chain (gray), the MG3 domain (blue) and the MG8 domain (green). A Cd^{2+} ion (wheat-colored sphere) is coordinated by the α'-chain and the MG3 domain. Glyco, glycosylation at Asn741. (c) Surface of C5a (red; residues 749–751 not presented) in two orientations differing by a vertical rotation of 180°. Residues within 4 Å of the rest of C5 are pink; six residues identified as being part of the C5a-C5aR interface[27] are wheat-colored. (d) Electron density around the convertase site. The nature and position of the Cd^{2+} ion can be verified from the anomalous-difference map (red density) contoured at 6 σ. A simulated annealing omit $2mF_o - DF_c$ electron-density map (gray) is contoured at 1 σ. Residues 262–264, 749–753 and the Cd^{2+} ion are omitted. *, residual density that may contain a water molecule linking the Cd^{2+} ion with Glu262. Modeling of Arg751 in this density places the positively charged side chain as a ligand to the Cd^{2+} ion and is therefore less likely.

have no expected structural homology with C5aR. The burial of receptor-interacting surface areas of C5a in C5 presumably helps to prevent interactions between C5 and C5aR before C5 cleavage.

The greater complexity of the C5 convertase relative to that of the C3 convertase is mirrored by the difficulty in generating C5a by proteolysis with nonspecific proteases relative to the generation of C3a from C3 (ref. 28). In C5, the convertase cleavage site Arg751-Leu752 is much more ordered than that of C3, with only residues 744–748 'upstream' being disordered (**Fig. 3**); in contrast, the cleavage site itself is disordered in both human and bovine C3 (refs. 19,20). Crude docking of a C2a molecule (the catalytic subunit of one of the two C5 convertases) onto C5 indicated that the residues flanking Arg751 must undergo a substantial conformational change to accommodate Arg751-Leu752 into the catalytic site of the protease and that the C345C domain cannot be located in the position it takes in the C5-1 molecule during C5 cleavage. In agreement with those results, small-angle X-ray scattering (SAXS) data showed that the C5 conformation noted in C5-1 is not the predominant conformational state in solution (discussed below). The conformation of the convertase site may be influenced by a nearby Cd^{2+} ion (**Fig. 3b,d**), but the inclusion of Cd^{2+} ions does not influence tryptic cleavage of C5 (L.S.-J., unpublished data). In the absence of the Cd^{2+} ion, Arg751 might engage in salt bridges with the highly conserved Glu262 and Asp264 (**Fig. 3b,d**), whereas in the crystal structure, it is kept in position by the main-chain atoms of Gly750.

In addition to the direct binding of Arg751-Leu752 to the catalytic sites of C2a or Bb, other regions in C5 interact with the C5 convertases. Recognition of C5 by C3b is a requirement for the cleavage of C5 by the C5 convertase[11]. Residues 1628–1633 in the C345C domain must be in direct contact with the C5 convertase, as a peptide mimicking this region prevents cleavage of C5 by the classical pathway convertase[17,29]; in addition, a C3b-binding site has been assigned to C5d[28] on the basis of antibody-inhibition studies. Other regions involved in convertase recognition may be identified from visualization of the residue conservation of the surface of C5. Many conserved residues in the C5d, CUB and the MG8 domains gather at the 'top' of the molecule (**Fig. 4a,b**). Additionally, a fairly large cavity with contributions from domains MG2, MG6, MG7, CUB and C5d (**Fig. 4c**) is likewise notably conserved. A similar cavity is present in C3 and most likely in C4 as well, but it is considerably smaller in C3 because of the closer approach of the MG7 domain, which in C5 is rotated 13° away from C5d relative to C3 (**Fig. 4d**). A smaller conserved patch formed by regions from MG1, MG5 and the linker region is also present at the 'bottom' of C5 and faces the same side of

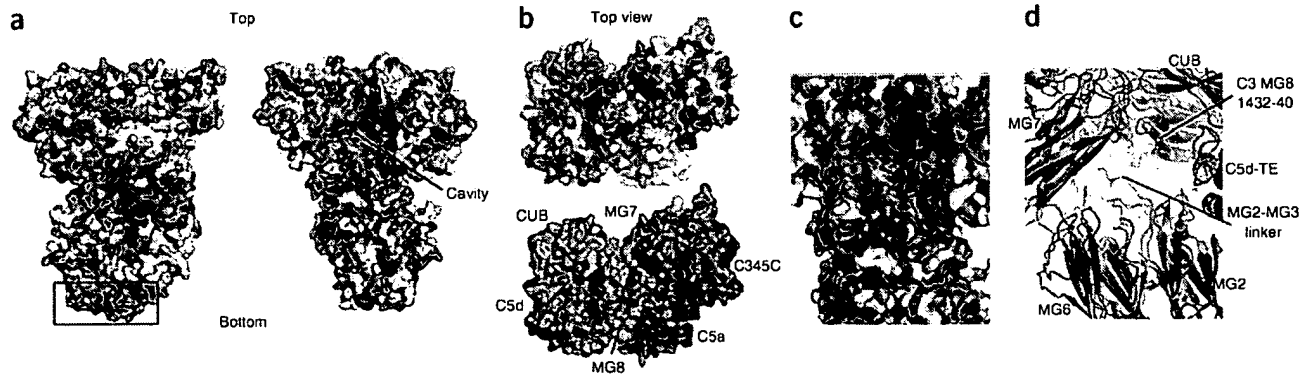

Figure 4 Conserved surface areas of C5. (a) In the two main orientations from **Figure 1**, orange areas are identical in seven C5 sequences, green areas are identical in six of these, and gray areas are identical in less than six sequences. Boxed area below outlines a highly conserved surface patch. (b) Above, top view of conserved residues in the superdomain of C5, which together with the nearby mobile C345C domain may form binding sites for C3b. Below, surface representation in the same orientation with the domains in colors as in **Figure 1**. (c) Enlargement of the large conserved cavity in the center of the molecule in a. (d) Cavity in C5 (teal) and in C3 (orange). Both c and d are in the same orientation.

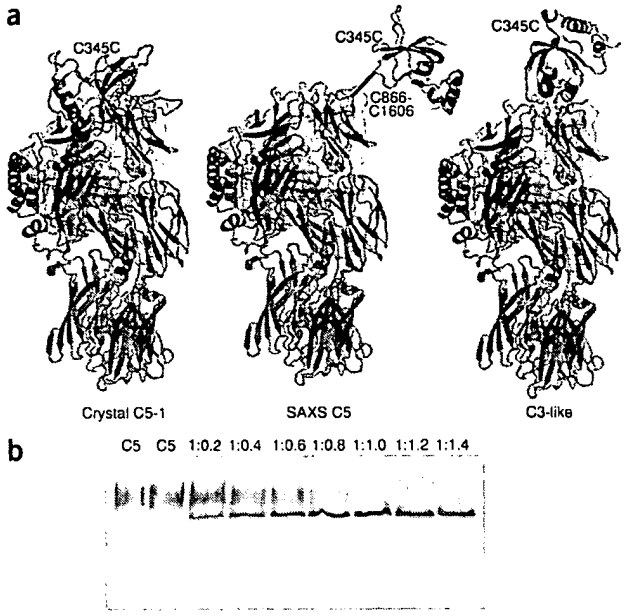

Figure 5 Solution structure of C5. (a) Left, C5-1 molecule from the crystal structure (teal, core C5; wheat, C345C domain); middle, C5 fitted to SAXS data with two rigid bodies, including the distance restraint Cys866-Cys1606; right, C5 modeled with the C345C domain in a C3-like location. (b) Native gel electrophoresis of the 'titration' of C5 with OmCI; above lanes, molar ratio of C5 and OmCI. Samples were incubated for 1 h at 37 °C before electrophoresis, except the far left lane, incubated for 1 h at 4 °C.

the molecule as C5a (**Fig. 4a**). Although these three areas are far apart and span almost all of C5, they may all be involved in recognition by the C5 convertase in combination with the region in the C345C domain known to be important for convertase action[29]. The convertase is a very large macromolecular complex with dimensions that must be even larger than those of C5.

The C5-OmCI complex

The soft tick complement inhibitor OmCI has been suggested to inhibit C5 cleavage by competing with the C345C domain and dislodging it from the C5 core, thereby preventing recognition of C5 by C5 convertase[30]. The crystal structure, native gel electrophoresis and our SAXS data indicated the opposite mechanism (**Fig. 5** and **Supplementary Fig. 3** online). In the absence of OmCI, the C345C domain is flexibly attached to the core of C5 in an exposed position different from that of either C5-1 or C3, consistent with the smeared C5 band obtained by native gel electrophoresis (**Fig. 5b**) and its activity in the crystals. In the presence of OmCI, the SAXS data showed that despite having a higher molecular weight, the complex has a smaller radius of gyration in solution than in the absence of OmCI, which indicates that the C345C domain is more closely associated with the core of C5 in the C5-OmCI complex. In agreement with those results, the complex formed a well-defined and faster migrating band in the native gel (**Fig. 5b**). 'Dummy' atom modeling of the C345C domain and OmCI in the C5-OmCI complex on the basis of the SAXS data suggested that they are located near each other at the distal end of the CUB-C5d-MG8 superdomain (**Supplementary Fig. 3d**). Surface plasmon resonance measurements (**Supplementary Fig. 3e**) supported the idea of direct interaction between OmCI and the core of C5, as the isolated C345C domain did not interact with OmCI in these experiments. Either contacts with the core of C5 are needed to induce the correct conformations in the C345C domain and OmCI for their mutual interaction to take place, or they do not interact directly. In the surface plasmon resonance experiments, OmCI and C345C were able to bind C5 and C7, respectively, which showed that they had maintained overall native conformations. Notably, C7 was able to interact with the C5-OmCI complex (**Supplementary Fig. 3e**), which suggested that the C7 recognition patch on the C345C domain remains exposed when OmCI is bound to C5. In support of the idea of proximity between OmCI and the C345C domain, the interaction between C7 and the C5-OmCI complex seemed to be blocked by OmCI-specific polyclonal antibodies.

Binding of the complement inhibitor Efb to C3 leads to more nonspecific cleavage of C3 by trypsin[31], but we noted the opposite effect after binding of OmCI to C5, as the C5-OmCI complex was cleaved more slowly by trypsin than was C5 alone (**Supplementary Fig. 4** online). The peptide bonds Lys879-Ser880 and Arg1392-Gly1393 in the MG7 and MG8 domains, respectively, are less accessible to trypsin cleavage in the C5-OmCI complex. Both these sites are in disordered unmodeled regions of the C5 structure, and although the 'dummy' atom modeling of the C5-OmCI complex suggested that OmCI could shield the Arg1392-Gly1393 bond directly, this is less likely for the Lys879-Ser880 peptide. This suggests an overall stabilization of the C5 α-chain in the C5-OmCI complex relative to that in C5. As the MG7 domain is linked by the anchor region through disulfide bridges to the C345C domain, the MG7 domain may become more tightly associated with the CUB-C5d-MG8 superdomain, as in C3 (**Fig. 4d**), after the locking of C345C in the C5-OmCI complex.

Collectively, our studies have shown a C345C domain that can adopt a variety of different locations relative to the C5 core. The solution-scattering data for C5 showed that the C345C domain is unlikely to be solely responsible for the interaction of C5b with other MAC subunits (**Supplementary Fig. 5** online). Given the flexible attachment to the rest of C5, this would probably not be sufficiently discriminatory against native C5 (discussed below).

DISCUSSION

The structures of C3, TEP and C5 have allowed us to deduce common principles of the structural properties of proteins in the α_2M superfamily. First, all the domains originally defined in C3, except for the C3-, C4- and C5-specific anaphylatoxin and C345C domains, are structurally conserved. Second, the packing of the CUB-C5d-MG8 domains is conserved in the uncleaved state of these proteins and is not dependent on the thioester. Instead, this domain arrangement protects the thioester very efficiently and is probably required for formation of the thioester[20]. Third, the quaternary structure of the MG1-6 superhelix is variable, and although it seems relatively rigid during the transition from C3-C3b to C3b-C3c[19,22,23], a substantial conformational change in the MG1-6 superhelix may occur in other members of the α_2M superfamily after proteolytic activation, as suggested by the structure of TEP[21]. The structures of C3 and C5 may be extrapolated to C4. The sequence identity is 26–29% for pairs of the three proteins; hence, C4 can be expected to show deviations from C3 or C5 of the same order of magnitude as those noted between C3 and C5. The core of C4 probably has a structure very similar to that of C3 and C5, and its C345C domain may be in a defined location, as in C3, or flexibly attached to the core, as in C5.

Our studies have shown that the C345C domain in C5 can be present in at least three different locations. In C5-1 of the crystal structure, it is located near C5a and blocks access to the convertase site, whereas in solution, the C345C domain makes little interaction with the core of C5 and does not block the convertase cleavage site. In

complex with OmCI, the domain seems less flexible and located closer to the core of C5, and in the C5-2 molecule of the crystal structure it is probably located in a C3-like location. The flexibility of the C345C domain may be important during convertase recognition of C5, in which the domain interacts directly with the convertase[17,29]. A requirement for C345C flexibility and accessibility also suggests that OmCI inhibits convertase action by stabilizing the C345C domain in a fixed position, and our trypsin digestion experiments have indicated that binding of OmCI also leads to an overall conformational stabilization of the C5 α-chain. How often the C345C domain comes near C5a as in the C5-1 molecule *in vivo* remains an open issue, as the interaction between the C345C domain and the C5-1 core seems to be strongly stabilized by crystal packing. A Cd^{2+} ion surrounded by His894 and Gln886 from the MG7 domain and Glu1589 from the C345C domain, all of which are highly conserved residues, is important in the interface. Whether a divalent ion binds here *in vivo* is unknown, but if absent, its function may be provided instead by electrostatic interactions and hydrogen bonds between side chains from the MG7 and the C345C domains.

When C5b is formed, it is present in a metastable conformation that must react within minutes with C6 to form the essentially irreversible C5bC6 complex[32], which further associates with C7. C5b aggregates in the absence of C6 (ref. 33), whereas C5 is highly soluble and monomeric, so the transition from C5 to C5b must expose new, large, surface-exposed interaction sites that contact C6 and C7, which suggests that the α-chain in C5 undergoes a substantial conformational change after cleavage in a way similar to the C3-to-C3b transition[19,22,23]. Electron microscopy of MAC has shown that club-shaped monomeric or dimeric leaflets extend 140–150 Å from the rim of the MAC barrel, which consists mainly of C5b[34]. The C6, C7, C8 and C9 components are embedded in the MAC tubule, whereas C5b can be released from MAC by chaotropic reagents[8]. Proteolytic stripping[35] and photolabeling[36] with a lipid-restricted photoprobe of C5bC6C7 has indicated that whereas the α′-chain of C5b is near the membrane, the β-chain is located at a greater distance from the membrane. The most likely overall orientation of C5b in the MAC complex is therefore with the β-chain pointing away from the MAC pore and the α′-chain pointing toward it. The C345C domain in C5 interacts with the factor I modules of C7 and possibly also with the C6 factor I modules[37], and the C7 factor I modules probably also interact with the C345C domain of C5bC6 during MAC assembly[38]. In agreement with a published model of C5b6 and C5bC6C7 (ref. 37), regions of C5 beyond the C345C domain must be involved in interaction with the other MAC subunits. Otherwise, the dislodged C345C domain we noted with solution scattering in C5 would probably not be sufficient to discriminate against MAC formation with native C5. In C3b, the CUB-thioester domain pair is fairly flexible relative to the rest of the molecule, and the thioester domain interacts with MG1 through a relatively small interaction area[22,23]. By negative-stain electron microscopy, it has been shown that a metastable intermediate of C3 obtained after thioester cleavage has the CUB and the thioester domains completely detached from the β-chain of C3 (ref. 25). In that study, a C3b-like conformation with the thioester domain contacting the β-chain was noted only after a specific time of incubation[25]. In C5, a similar flexibility may be used to propel the C5d domain toward the C345C domain and the other MAC subunits, rather than toward the MG1 domain, but a C3b-like conformation may develop if C5b fails to initiate MAC assembly.

There is a considerable need for therapeutic agents to block undesired complement activation in various disease conditions, including ischemia, paroxysmal nocturnal hemoglobinuria, systemic lupus erythematosus and inflammation[14,15], and to prevent rejection of transplanted organs[39]. In this context, C5 is an important target, as a C5 inhibitor selectively allows inhibition of the C5b and C5a-mediated responses while leaving the rest of complement unaffected. OmCI is not the only possible C5 inhibitor being investigated. The complement-specific drug eculizumab is an antibody directed against C5 (ref. 15) and is an effective agent against paroxysmal nocturnal hemoglobinuria. Combination therapy with this antibody and cyclosporin also results in long-term graft survival in a mouse cardiac allograft model[40], which suggests its potential usefulness in clinical transplantation. The structure of C5 represents a unique opportunity for accurately identifying surface patches on the molecules that might be targeted for the development of other C5 inhibitors. The example of OmCI shows that binding of a molecule to regions of C5 distant from the cleavage site can lead to convertase resistance due to rearrangement and/or stabilization of the structure or steric hindrance with the convertase.

METHODS

Purification and characterization. C5 was purified as described[41] or as follows, at 4 °C unless otherwise stated. Three aliquots of human plasma (300 ml each) were separately mixed with an equal volume of buffer A (20 mM Tris, 20 mM NaCl, 5 mM EDTA, 2 mM benzamidine and 200 μg/l of pancreatic trypsin inhibitor, pH 7.7). The plasma portions were separately precipitated in the 2–7% PEG 6000 fraction and were centrifuged for 15 min at 4,400*g*. The precipitates were resuspended in 100 ml buffer A and were centrifuged. Supernatants were sequentially loaded on a DEAE Sepharose Fast Flow column (5 cm × 50 cm) equilibrated in buffer A. Between loadings, the column was washed with 100 ml buffer A. The column was washed with three volumes of buffer A and samples were eluted with a 2,000-ml linear gradient of 20–300 mM NaCl. Pooled fractions were loaded on a Sephacryl S-300 (5 cm × 100 cm) equilibrated in buffer B (25 mM KH_2PO_4, 100 mM KCl, 25 mM ε-amino-caproic acid and 200 μg/l of pancreatic trypsin inhibitor, pH 7.4). Fractions containing C5 were loaded on a Hydroxyapatite HT Biogel column (5 cm × 15 cm; Bio-Rad) and were washed with 300 ml buffer B alone and 500 ml buffer B containing 2 M NaCl. Bound C5 desorbed from the column when the ionic strength was decreased and was eluted with 120 ml buffer B. Pooled C5-containing fractions were dialyzed against 20 mM HEPES and 100 mM NaCl, pH 7.5, were applied to a Mono Q 10/100 column and were eluted at 20 °C with a 44-ml linear gradient of 20–750 mM NaCl. Fractions containing C5 were mixed with an equal volume of 20 mM Tris and 1 M Na_2SO_4, pH 7.7, then were loaded on a 9-ml Source 15-Phe column equilibrated in 20 mM Tris and 0.5 M Na_2SO_4, pH 7.7, at 20 °C and were eluted with a 60-ml linear gradient of 0.5–0 M Na_2SO_4. For native gel electrophoresis of C5, 15 μg C5 in 20 mM HEPES and 100 mM NaCl, pH 7.2, was incubated for 1 h at 37 °C with increasing molar ratios of OmCI. Samples were loaded on a 10–20% standard Tris-glycine gel prepared without SDS, were separated by electrophoresis for 2 h at 10 mA and were visualized by staining with Coomassie brilliant blue G-250. For trypsin digestion, 100 μl C5 (1 mg/ml in 20 mM HEPES and 100 mM NaCl, pH 7.2) was mixed with 100 μl trypsin (0.01 mg/ml) purified on a benzamidine Sepharose column (assumed to be 50% active at time of use). The mixture was incubated at 20 °C, and 20-μl samples were removed at intervals and mixed with 1 μg pancreatic trypsin inhibitor. Prewarmed SDS sample buffer containing dithiothreitol was added and samples were incubated for 3 min at 100 °C. A volume of 20 μl was loaded on 10–20% SDS gradient gels. In one experiment, C5 was mixed with OmCI (1.8 molar excess) before the addition of trypsin.

Surface plasmon resonance. Measurements were made on a Biacore 2000 with reagents supplied by the same company. C5 and C7 were from Calbiochem. Recombinant OmCI, polyclonal rabbit antibody to OmCI IgG and recombinant C5-C345C were produced as described[13,42]. OmCI and C345C were immobilized by amine coupling to a Biacore sensor chip CM5 as recommended by Biacore. All experiments were done at 20 °C in 0.01 M HEPES, pH 7.4,

0.15 M NaCl and 0.005% (vol/vol) surfactant P20. Analyte solutions were passed through the flow cells sequentially at a flow rate of 20 μl per minute.

SAXS. Protein in 20 mM HEPES, pH 7.8, and 100 mM NaCl was concentrated to 5 mg/ml. SAXS measurements were made with a laboratory-based instrument at the University of Aarhus. For both C5 and the C5-OmCI complex sample, a series of concentrations (1–5 mg/ml) were measured for control of aggregation-interaction effects. The SUPERSAXS package was used for background subtraction and all necessary normalizations (C.L.P.O. and J.S.P., unpublished data). Data were normalized to an absolute scale with a sample of pure water as the primary standard (experimental points, **Supplementary Fig. 3**). The pair distance distribution function for the experimental data (data not shown) was calculated by the indirect Fourier transformation method. For C5, the radius of gyration R_g was 46.2 ± 0.3 Å and the maximum dimension was about 150 Å. For the C5-OmCI complex, R_g was 45.4 ± 0.2 Å and the maximum dimension was about 143 Å. As atomic-resolution structures were available for the core C5 residues 20–1515 and the C345C domain, rigid-body refinement with SASREF software[43] was used for modeling of the solution state of C5. Residues 1516–1540 had variable conformations in C5-1, C5-2 and the nuclear magnetic resonance structure of the C345C domain and were therefore omitted from the rigid-body refinements. The known substructures were used as input to the program together with atomic constraints relating the domains. After the minimization, a constant background was added to the theoretical fit with SUPERSAXS by a least-squares procedure. The addition of a constant background corrects for possible random fluctuation in electron density on the protein structure, flexibility of the domains, and errors in buffer subtraction not accounted for by SASREF. On the basis of the crystal structures of C3 and C5-1 in which the C345C can be located, the distances between the C_α positions in Cys866 in the C5 core and the Cys1606 in the C345C domain were restrained to below 20 Å (**Fig. 5a**). These two residues do not form a disulfide bridge but engage in disulfide bridges with Cys1527 and Cys1532, respectively, in the anchor region (**Supplementary Fig. 1c**). The equivalent distance in the crystal structures is 15 Å. Ten independent rigid-body refinements gave an almost identical orientation of the C345C domain (**Supplementary Fig. 3c**). The background corrected fit of the model to the experimental scattering curve is $\chi = 1.46$ (**Fig. 5a** and **Supplementary Fig. 3a**). The C5-1 molecule from the crystal structure fits with $\chi = 2.0$, whereas a modeled C5 molecule with the C345C domain in a place similar to that of C3 (**Fig. 5a**) fits with $\chi = 1.62$. For the C5-OmCI complex the C345C domain and OmCI were modeled as 'dummy' atoms with the BUNCH program[43] (**Supplementary Fig. 3d**).

Crystallization and soaking. Diffraction data were collected as described[41], but 10 μM Cd^{2+} was added to the cryoprotecting buffer to further stabilize the native crystals and the NaI-derivatized crystal, which resulted in improvement of the resolution[44]. Cd^{2+} was replaced with either Gd^{2+} or Sm^{2+} for the derivatives (**Supplementary Table 1**). Native data were collected at the Max-lab 711 beamline at $\lambda = 0.989$ Å. Data from crystals derivatized with Gd^{2+} or Sm^{2+} were collected at a rotating anode with $\lambda = 1.5418$ Å from crystals with maximum dimensions up to 1,500 μm (ref. 41). Later, these crystals could not be reproduced, so the NaI data were collected at the European Synchroton Radiation Facility beamline ID23-1 with $\lambda = 1.7712$ Å from crystals with maximum dimensions of 500 μm. These crystals were produced by concentration of the protein to 10 mg/ml in 100 mM NaCl and 20 mM HEPES, pH 7.8. For vapor-diffusion crystallization, proteins were mixed at a ratio of 2:1 with reservoir solution consisting of 100 mM NaCl and 1.5–3 mM 2-(*N*-morpholino)ethanesulfonic acid, pH 5.5, and were incubated at 4 °C. All data were processed with XDS software[45].

Structure determination. The space group of the C5 crystals is $P3_1$, but with a rotation axis of almost exactly twofold relating the two copies of the C5 core to each other, and with the C345C domain of C5-1 placed directly on this axis (**Supplementary Fig. 1b**). Data reduction is not sufficient to distinguish the space groups $P3_1$ and $P3_121$ (**Table 1**). For these reasons, the structure of the C5 core was first determined in $P3_121$ corresponding to the application of strict noncrystallographic symmetry restraints in $P3_1$. An initial set of phases in $P3_121$ was obtained by molecular replacement with PHASER software[46] with two independent search models derived from bovine C3. These phases were used to locate the samarium, gadolinium and iodide sites in anomalous diffraction data (**Table 1**). Experimental MIRAS phases were calculated with the SHARP program[47] with B factors fixed to 80 Å^2. Further sites were added at the location of positive peaks of the SHARP log-likelihood gradient anomalous maps. A total of 20, 23 and 13 sites were located in the samarium, gadolinium and iodide derivatives, respectively. The final combined figure of merit in the resolution range 50–4.5 was 0.36 for the centric reflections and 0.39 for the acentric reflections. Domains not found by molecular replacement (C5a, MG1, MG3 and MG4) were docked 'by hand' in the solvent-flipped map generated after the experimental phasing. Because of the low resolution of the experimental phases and the low sequence identity of 28% between C3 and C5, many cycles of iterative rebuilding with the O program[48], refinement with the crystallography and nuclear magnetic resonance system[49], a combination of experimental and model phases, and solvent flipping were required. Initially, model phases for polyalanine models were used and, later, omit model phases were used for each domain, so that each domain was built into density not containing model-phase contribution from the domain itself. Composite annealing-omit maps were used for rebuilding as well. The structure was refined with density-modified combined phases as restraints. From an R_{free} of 35%, the structure was refined with the phenix.refine program[50] without phase restraints. Five and nine Cd^{2+} ions bound to C5 were located from the weak anomalous signal in the native data in space groups $P3_121$ and $P3_1$, respectively. At an R_{free} of 29.2%, the symmetry was switched to $P3_1$ with simultaneous symmetry expansion of the test set from $P3_121$ to $P3_1$ with the SFTOOLS program. After symmetry expansion, the C345C domain was located in both C5-1 and C5-2 by molecular replacement but was included in the final model only for C5-1. In $P3_1$, the structure was refined with noncrystallographic symmetry restraints applied domain-wise. In the final model, 74.9% of the residues were in the most-favored regions of the Ramachandran plot, 24.6% were in additionally allowed regions and 0.5% were in disallowed regions.

Accession code. Research Collaboratory for Structural Bioinformatics protein data bank: coordinates and structure factors for C5, 3CU7.

Note: Supplementary information is available on the Nature Immunology website.

ACKNOWLEDGMENTS

We thank L. Kristensen for technical assistance; C. Andersen for help with figures; the staff of Elettra, Max-lab, the European Synchrotron Radiation Facility, and the Swiss Light Source for help with data collection; R. Ogata (Torrey Pines Institute for Molecular Studies) for C5-C345C; and P. Morgan (Cardiff University) for polyclonal rabbit antibody to OmCI IgG. Supported by the Danish Natural Science Research Council, the Novo Nordisk Foundation, the Carlsberg Foundation, the Danish National Research Foundation and Dansync (G.R.A., L.J., J.S.P. and L.S.-J.); and by the British Biotechnology and Biological Sciences Research Council and the National Environmental Research Council (S.M.L., P.R. and M.A.N.).

AUTHOR CONTRIBUTIONS

F.F., crystallization, data collection, structure determination, refinement and analysis, and manuscript preparation; N.S.L. and L.S.-J., purification and analysis of C5 and C5-OmCI; P.R. and S.M.L., experimental phasing and molecular replacement; M.A.N., surface plasmon resonance experiments and preparation of OmCI; C.L.P.O. and J.S.P., SAXS analysis; L.J. and R.D., initial protein purification, crystallization and data collection; and G.R.A., conceptual design, structure analysis and manuscript preparation.

Published online at http://www.nature.com/natureimmunology/
Reprints and permissions information is available online at http://npg.nature.com/reprintsandpermissions/

1. Gerard, N.P. & Gerard, C. The chemotactic receptor for human C5a anaphylatoxin. *Nature* **349**, 614–617 (1991).
2. Gerard, C. & Gerard, N.P. C5A anaphylatoxin and its seven transmembrane-segment receptor. *Annu. Rev. Immunol.* **12**, 775–808 (1994).
3. Gerard, N.P. *et al.* An anti-inflammatory function for the complement anaphylatoxin C5a-binding protein, C5L2. *J. Biol. Chem.* **280**, 39677–39680 (2005).
4. Chen, N.J. *et al.* C5L2 is critical for the biological activities of the anaphylatoxins C5a and C3a. *Nature* **446**, 203–207 (2007).
5. Podack, E.R., Esser, A.F., Biesecker, G. & Muller-Eberhard, H.J. Membrane attack complex of complement: a structural analysis of its assembly. *J. Exp. Med.* **151**, 301–313 (1980).

6. Ramm, L.E., Whitlow, M.B. & Mayer, M.M. Size of the transmembrane channels produced by complement proteins C5b-8. *J. Immunol.* **129**, 1143–1146 (1982).
7. Podack, E.R., Tschoop, J. & Muller-Eberhard, H.J. Molecular organization of C9 within the membrane attack complex of complement. Induction of circular C9 polymerization by the C5b-8 assembly. *J. Exp. Med.* **156**, 268–282 (1982).
8. Podack, E.R. Molecular composition of the tubular structure of the membrane attack complex of complement. *J. Biol. Chem.* **259**, 8641–8647 (1984).
9. Kinoshita, T. *et al.* C5 convertase of the alternative complement pathway: covalent linkage between two C3b molecules within the trimolecular complex enzyme. *J. Immunol.* **141**, 3895–3901 (1988).
10. Takata, Y. *et al.* Covalent association of C3b with C4b within C5 convertase of the classical complement pathway. *J. Exp. Med.* **165**, 1494–1507 (1987).
11. Vogt, W., Schmidt, G., Von Buttlar, B. & Dieminger, L. A new function of the activated third component of complement: binding to C5, an essential step for C5 activation. *Immunology* **34**, 29–40 (1978).
12. Nunn, M.A. *et al.* Complement inhibitor of C5 activation from the soft tick *Ornithodoros moubata*. *J. Immunol.* **174**, 2084–2091 (2005).
13. Hepburn, N.J. *et al.* In vivo characterization and therapeutic efficacy of a C5-specific inhibitor from the soft tick *Ornithodoros moubata*. *J. Biol. Chem.* **282**, 8292–8299 (2007).
14. Ricklin, D. & Lambris, J.D. Complement-targeted therapeutics. *Nat. Biotechnol.* **25**, 1265–1275 (2007).
15. Rother, R.P., Rollins, S.A., Mojcik, C.F., Brodsky, R.A. & Bell, L. Discovery and development of the complement inhibitor eculizumab for the treatment of paroxysmal nocturnal hemoglobinuria. *Nat. Biotechnol.* **25**, 1256–1264 (2007).
16. DiScipio, R.G. The conversion of human complement component C5 into fragment C5b by the alternative-pathway C5 convertase. *Biochem. J.* **199**, 497–504 (1981).
17. Bramham, J. *et al.* Functional insights from the structure of the multifunctional C345C domain of C5 of complement. *J. Biol. Chem.* **280**, 10636–10645 (2005).
18. Zuiderweg, E.R., Nettesheim, D.G., Mollison, K.W. & Carter, G.W. Tertiary structure of human complement component C5a in solution from nuclear magnetic resonance data. *Biochemistry* **28**, 172–185 (1989).
19. Janssen, B.J. *et al.* Structures of complement component C3 provide insights into the function and evolution of immunity. *Nature* **437**, 505–511 (2005).
20. Fredslund, F. *et al.* The structure of bovine complement component 3 reveals the basis for thioester function. *J. Mol. Biol.* **361**, 115–127 (2006).
21. Baxter, R.H. *et al.* Structural basis for conserved complement factor-like function in the antimalarial protein TEP1. *Proc. Natl. Acad. Sci. USA* **104**, 11615–11620 (2007).
22. Janssen, B.J., Christodoulidou, A., McCarthy, A., Lambris, J.D. & Gros, P. Structure of C3b reveals conformational changes that underlie complement activity. *Nature* **444**, 213–216 (2006).
23. Wiesmann, C. *et al.* Structure of C3b in complex with CRIg gives insights into regulation of complement activation. *Nature* **444**, 217–220 (2006).
24. Perkins, S.J., Smith, K.F., Nealis, A.S., Lachmann, P.J. & Harrison, R.A. Structural homologies of component C5 of human complement with components C3 and C4 by neutron scattering. *Biochemistry* **29**, 175–180 (1990).
25. Nishida, N., Walz, T. & Springer, T.A. Structural transitions of complement component C3 and its activation products. *Proc. Natl. Acad. Sci. USA* **103**, 19737–19742 (2006).
26. Isaac, L. *et al.* Native conformations of human complement components C3 and C4 show different dependencies on thioester formation. *Biochem. J.* **329**, 705–712 (1998).
27. Hagemann, I.S., Miller, D.L., Klco, J.M., Nikiforovich, G.V. & Baranski, T.J. Structure of the complement factor 5a (C5a) receptor-ligand complex studied by disulfide trapping and molecular modeling. *J. Biol. Chem.* **283**, 7763–7775 (2008).
28. DiScipio, R.G. Formation and structure of the C5b-7 complex of the lytic pathway of complement. *J. Biol. Chem.* **267**, 17087–17094 (1992).
29. Sandoval, A., Ai, R., Ostresh, J.M. & Ogata, R.T. Distal recognition site for classical pathway convertase located in the C345C/netrin module of complement component C5. *J. Immunol.* **165**, 1066–1073 (2000).
30. Roversi, P. *et al.* The structure of OMCI, a novel lipocalin inhibitor of the complement system. *J. Mol. Biol.* **369**, 784–793 (2007).
31. Hammel, M. *et al.* A structural basis for complement inhibition by *Staphylococcus aureus*. *Nat. Immunol.* **8**, 430–437 (2007).
32. DiScipio, R.G., Linton, S.M. & Rushmere, N.K. Function of the factor I modules (FIMS) of human complement component C6. *J. Biol. Chem.* **274**, 31811–31818 (1999).
33. DiScipio, R.G., Smith, C.A., Muller-Eberhard, H.J. & Hugli, T.E. The activation of human complement component C5 by a fluid phase C5 convertase. *J. Biol. Chem.* **258**, 10629–10636 (1983).
34. Tschopp, J., Podack, E.R. & Muller-Eberhard, H.J. Ultrastructure of the membrane attack complex of complement: detection of the tetramolecular C9-polymerizing complex C5b-8. *Proc. Natl. Acad. Sci. USA* **79**, 7474–7478 (1982).
35. Bhakdi, S., Tranum-Jensen, J. & Klump, O. The terminal membrane C5b-9 complex of human complement. Evidence for the existence of multiple protease-resistant polypeptides that form the trans-membrane complement channel. *J. Immunol.* **124**, 2451–2457 (1980).
36. DiScipio, R.G., Chakravarti, D.N., Muller-Eberhard, H.J. & Fey, G.H. The structure of human complement component C7 and the C5b-7 complex. *J. Biol. Chem.* **263**, 549–560 (1988).
37. Thai, C.T. & Ogata, R.T. Complement components C5 and C7: recombinant factor I modules of C7 bind to the C345C domain of C5. *J. Immunol.* **173**, 4547–4552 (2004).
38. Thai, C.T. & Ogata, R.T. Recombinant C345C and factor I modules of complement components C5 and C7 inhibit C7 incorporation into the complement membrane attack complex. *J. Immunol.* **174**, 6227–6232 (2005).
39. Sacks, S.H., Chowdhury, P. & Zhou, W. Role of the complement system in rejection. *Curr. Opin. Immunol.* **15**, 487–492 (2003).
40. Wang, H. *et al.* Prevention of acute vascular rejection by a functionally blocking anti-C5 monoclonal antibody combined with cyclosporine. *Transplantation* **79**, 1121–1127 (2005).
41. Discipio, R.G. *et al.* Crystallization of human complement component C5. *Acta Crystallogr.* **D54**, 643–646 (1998).
42. Thai, C.T. & Ogata, R.T. Expression and characterization of the C345C/NTR domains of complement components C3 and C5. *J. Immunol.* **171**, 6565–6573 (2003).
43. Petoukhov, M.V. & Svergun, D.I. Global rigid body modeling of macromolecular complexes against small-angle scattering data. *Biophys. J.* **89**, 1237–1250 (2005).
44. Jenner, L. *Structural Studies of Proteins from the α-Macroglobulin Superfamily.* Thesis, Univ. Aarhus (2000).
45. Kabsch, W. in *International Tables for Crystallography*, Vol. F (eds. Rossmann, M.G. & Arnold, E.) Ch. 25.22.29. (Kluwer Academic, Dordrecht, 2001).
46. Storoni, L.C., McCoy, A.J. & Read, R.J. Likelihood-enhanced fast rotation functions. *Acta Crystallogr.* **D60**, 432–438 (2004).
47. Bricogne, G., Vonrhein, C., Flensburg, C., Schiltz, M. & Paciorek, W. Generation, representation and flow of phase information in structure determination: recent developments in and around SHARP 2.0. *Acta Crystallogr.* **D59**, 2023–2030 (2003).
48. Jones, T.A., Cowan, S., Zou, J.-Y. & Kjeldgaard, M. Improved methods for building protein models in electron density maps and the location of errors in these models. *Acta Crystallogr.* **A47**, 110–119 (1991).
49. Brunger, A.T. *et al.* Crystallography & NMR system: A new software suite for macromolecular structure determination. *Acta Crystallogr.* **D54**, 905–921 (1998).
50. Adams, P.D. *et al.* PHENIX: building new software for automated crystallographic structure determination. *Acta Crystallogr.* **D58**, 1948–1954 (2002).

Erratum: Structure of and influence of a tick complement inhibitor on human complement component 5

Folmer Fredslund, Nick S Laursen, Pietro Roversi, Lasse Jenner, Cristiano L P Oliveira, Jan S Pedersen, Miles A Nunn, Susan M Lea, Richard Discipio, Lars Sottrup-Jensen & Gregers R Andersen

Nature Immunology 9, 753–760 (2008); published online 8 June 2008; corrected after print 20 June 2008

In the version of this article initially published, the numbers in the 'Rsym' row in Table 1 are in the wrong columns. The error has been corrected in the HTML and PDF versions of the article.

EXHIBIT F